El observatorio LAGO

Mauricio Suárez Duŕan
Ecuador, Sept. 2025

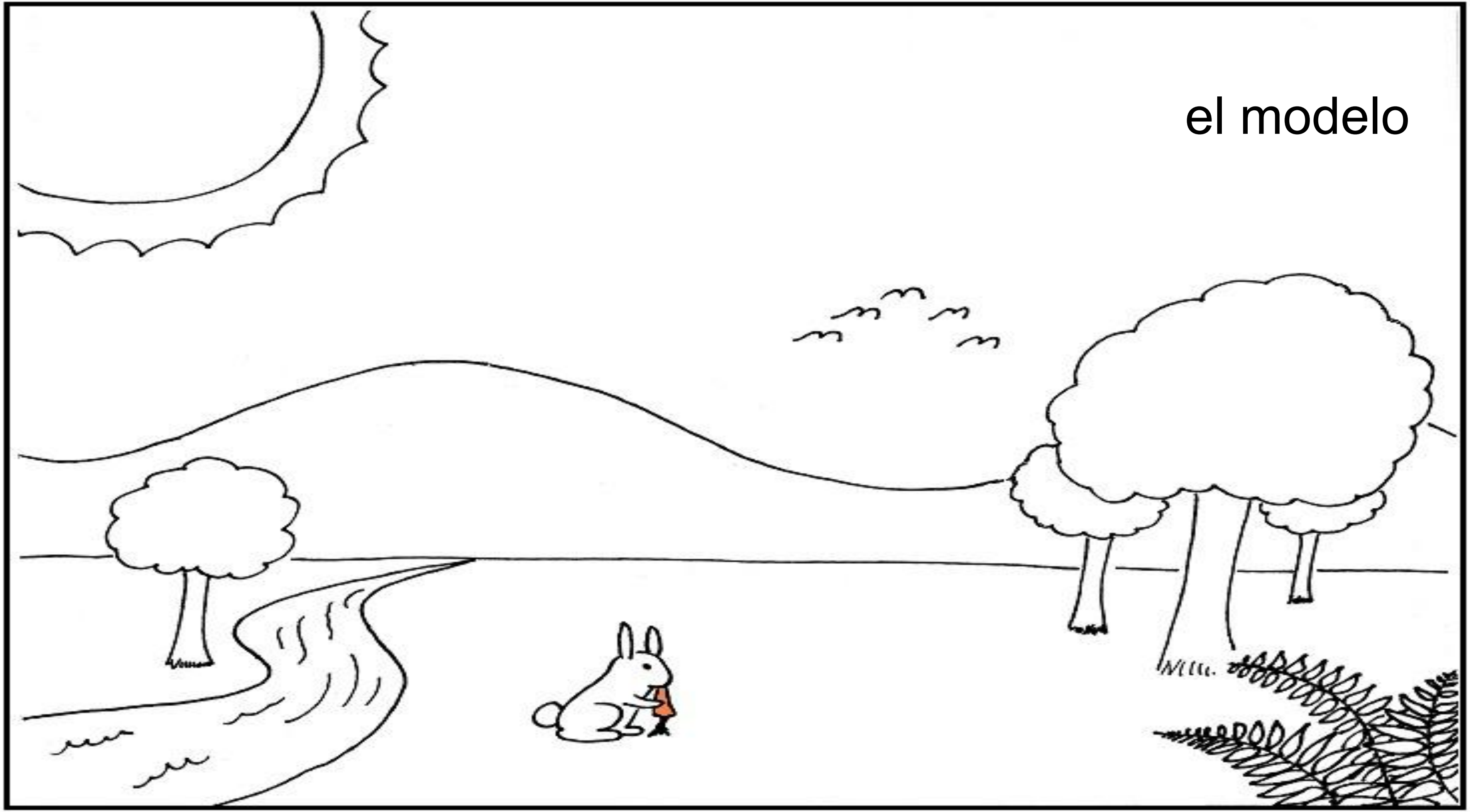
el modelo

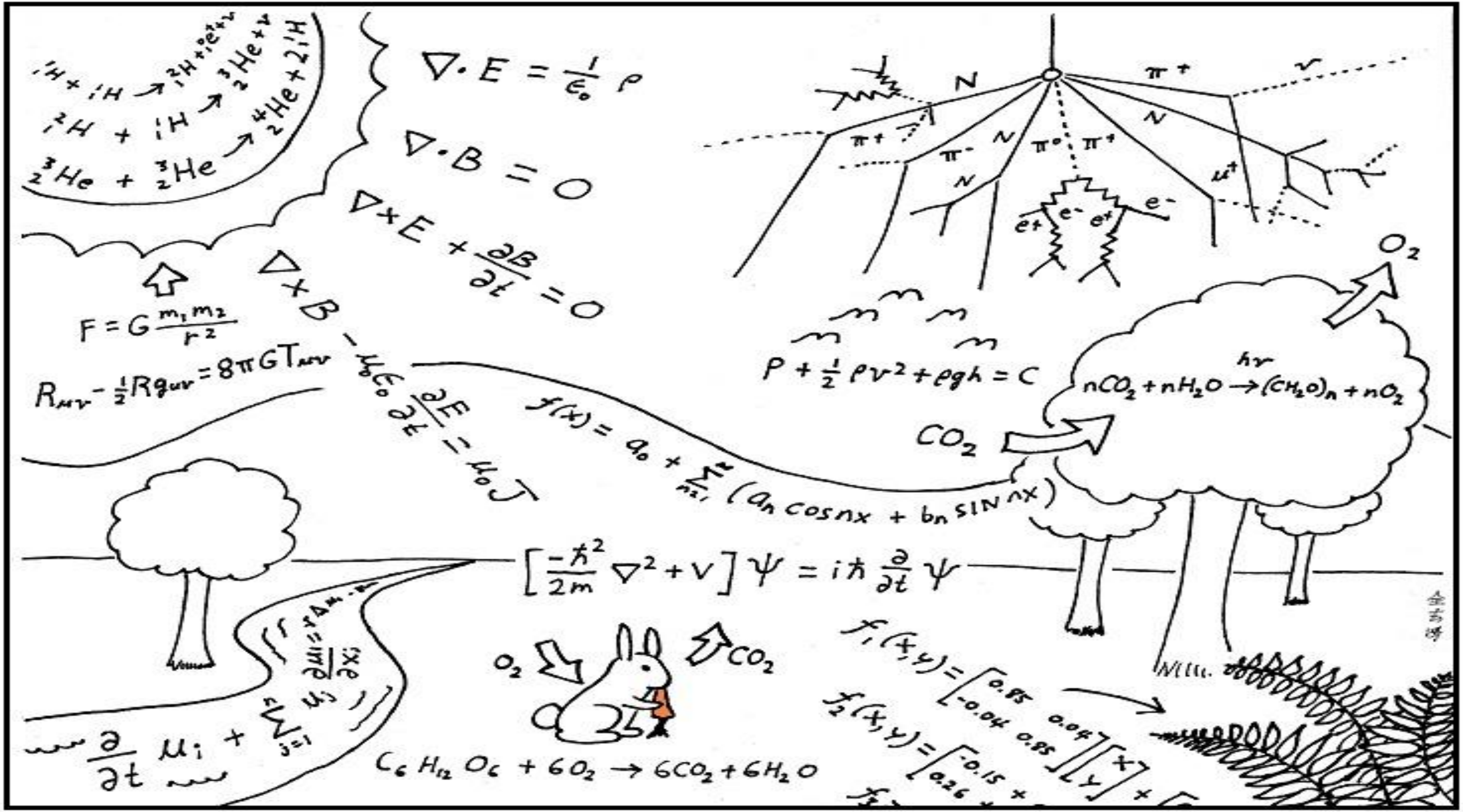

$^1_1H + ^1_1H \rightarrow ^2_1H + ^0_1e^+ + \nu$
$^2_1H + ^1_1H \rightarrow ^3_2He + \gamma$
$^3_2He + ^3_2He \rightarrow ^4_2He + 2^1_1H$
$\nabla \cdot E = \frac{1}{\epsilon_0}\rho$
$\nabla \cdot B = 0$
$\nabla \times E + \frac{\partial B}{\partial t} = 0$
$\nabla \times B - \mu_0\epsilon_0\frac{\partial E}{\partial t} = \mu_0 J$
$F = G\frac{m_1 m_2}{r^2}$
$R_{\mu\nu} - \frac{1}{2}Rg_{\mu\nu} = 8\pi G T_{\mu\nu}$
N
π^+
π^-
π^0
μ^+
e^-
e^+
$P + \frac{1}{2}\rho v^2 + \rho g h = C$
O_2
$nCO_2 + nH_2O \xrightarrow{h\nu} (CH_2O)_n + nO_2$
CO_2
$f(x) = a_0 + \sum_{n=1}^{\infty}(a_n \cos nx + b_n \sin nx)$
$\left[\frac{-\hbar^2}{2m}\nabla^2 + V\right]\Psi = i\hbar\frac{\partial}{\partial t}\Psi$
$\frac{\partial}{\partial t}u_i + \sum_{j=1}^{n} u_j \frac{\partial u_i}{\partial x_j} = r\Delta u$
O_2
CO_2
$C_6H_{12}O_6 + 6O_2 \rightarrow 6CO_2 + 6H_2O$
$f_1(x,y) = \begin{bmatrix} 0.85 & 0.04 \\ -0.04 & 0.85 \end{bmatrix}\begin{bmatrix} x \\ y \end{bmatrix} +$
$f_2(x,y) = \begin{bmatrix} -0.15 & \\ 0.26 & \end{bmatrix}$

el Universo extremo

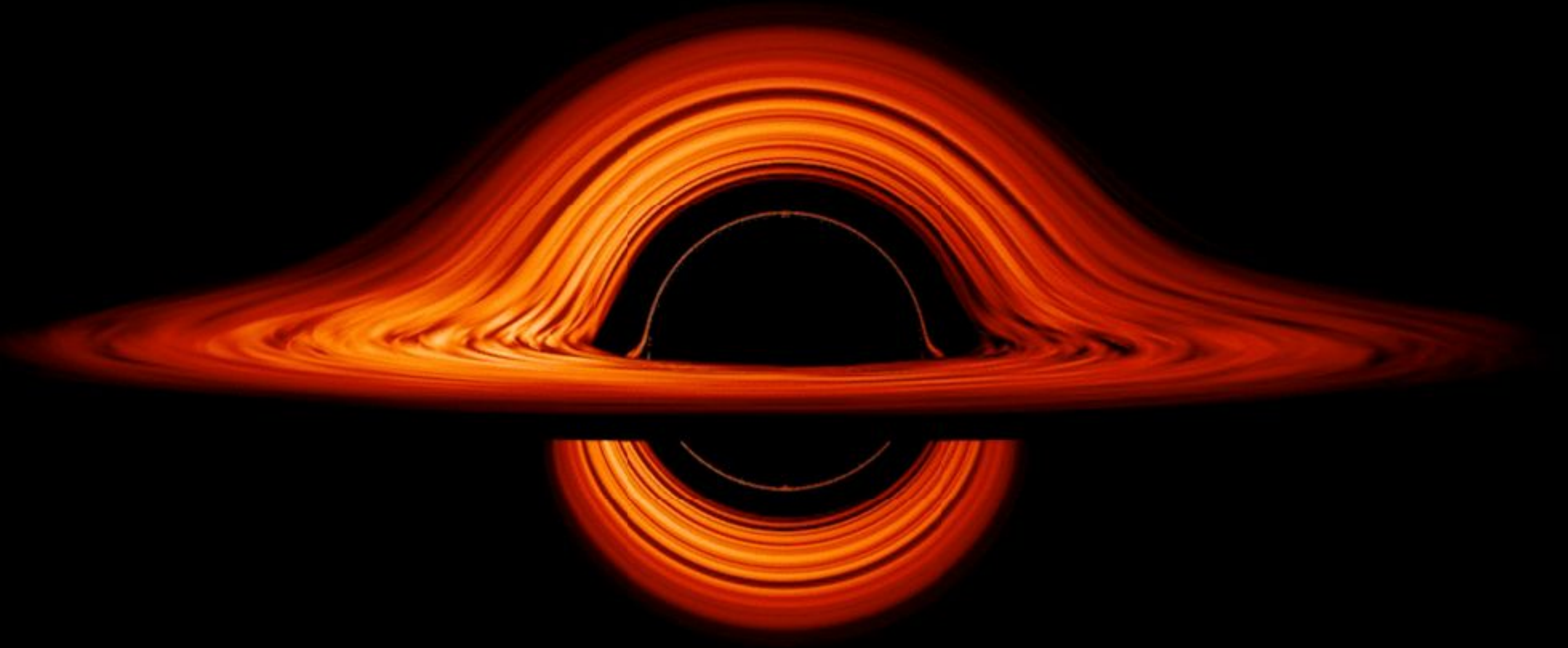


lluvias atmosféricas extensas

Lluvias atmosféricas extendidas: cada rayo cósmico interactúa con la atmósfera produciendo una cascada con hasta >10^{10} (>10 000 000 000) partículas secundarias

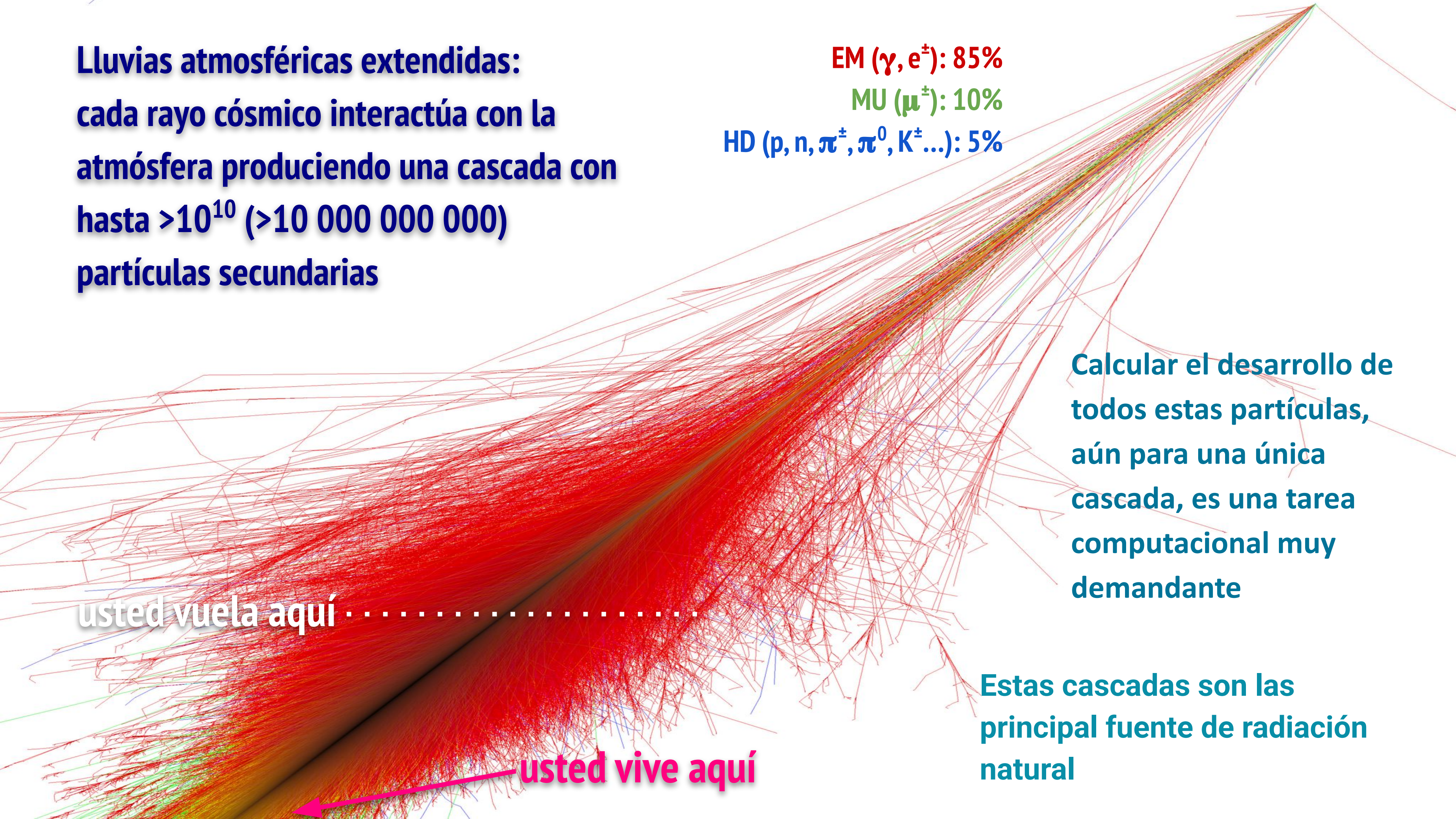

Calcular el desarrollo de todos estas partículas, aún para una única cascada, es una tarea computacional muy demandante

Estas cascadas son las principal fuente de radiación natural

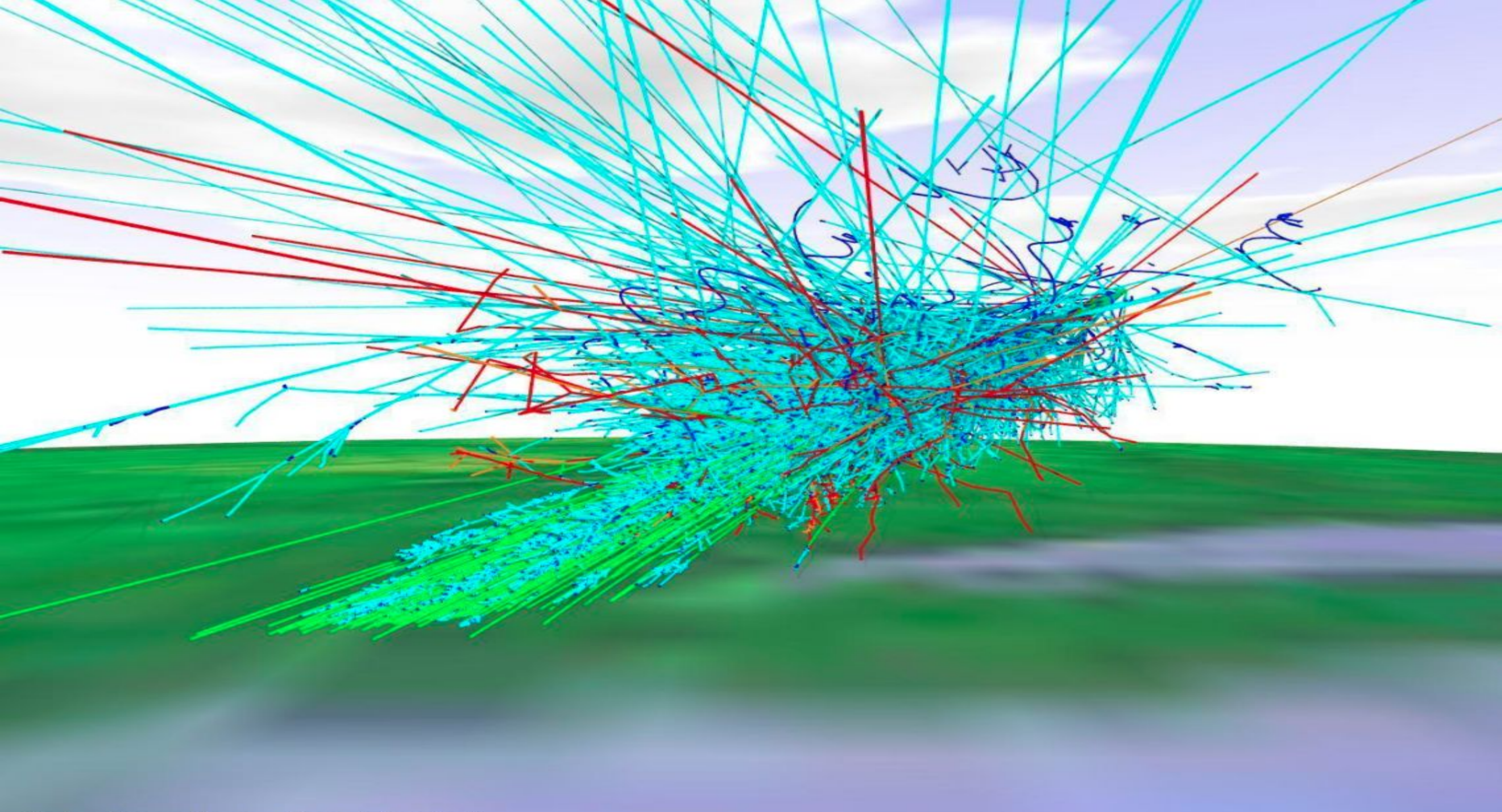

Hajo Drescher, Frankfurt U.

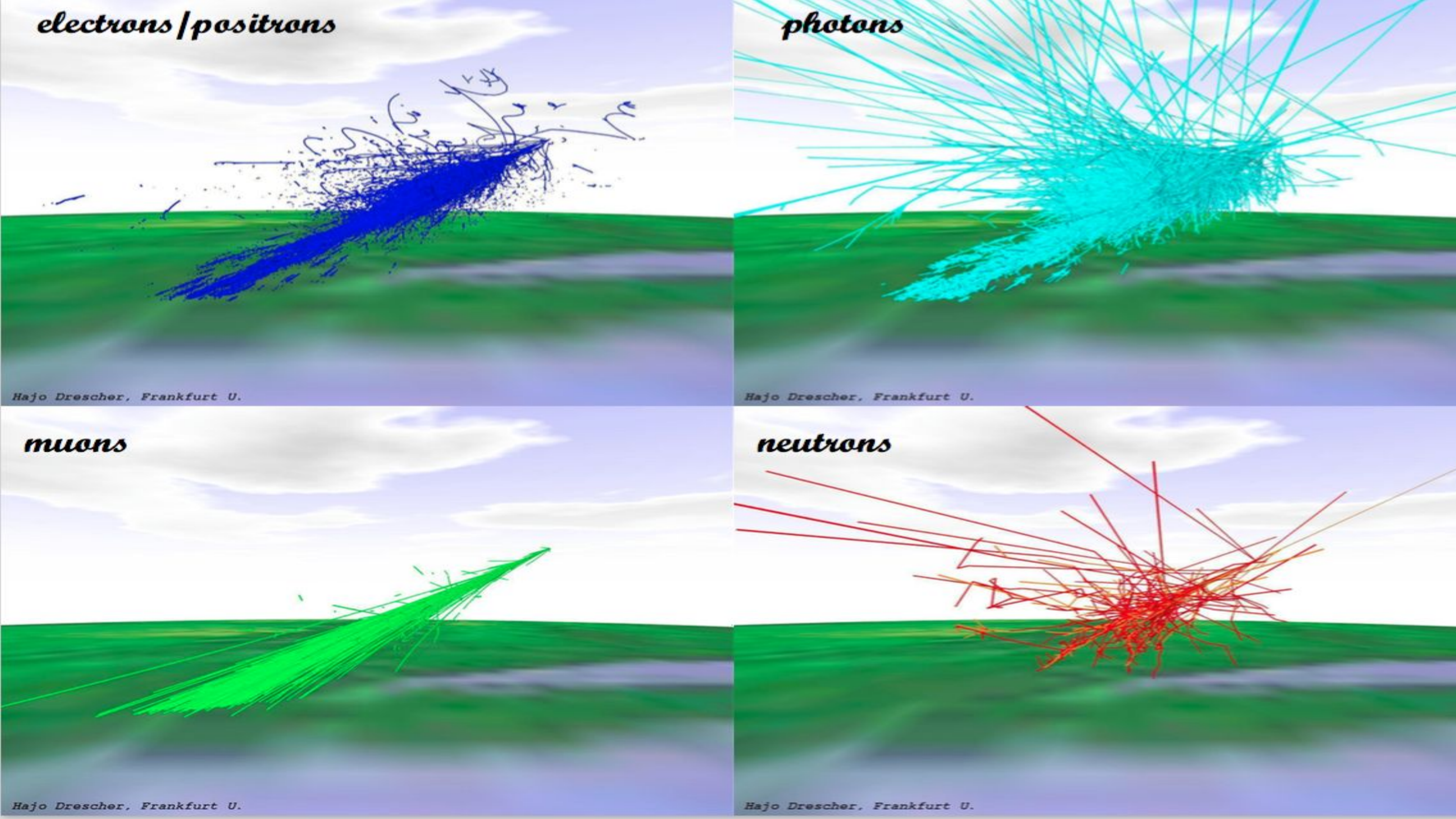
electrons/positrons
Hajo Drescher, Frankfurt U.
photons
Hajo Drescher, Frankfurt U.
muons
Hajo Drescher, Frankfurt U.
neutrons
Hajo Drescher, Frankfurt U.

LAGO
the Latin American Giant Observatory

LAGO

LAGO is a giant network of astroparticle detectors at global scale, currently operating in 11 countries

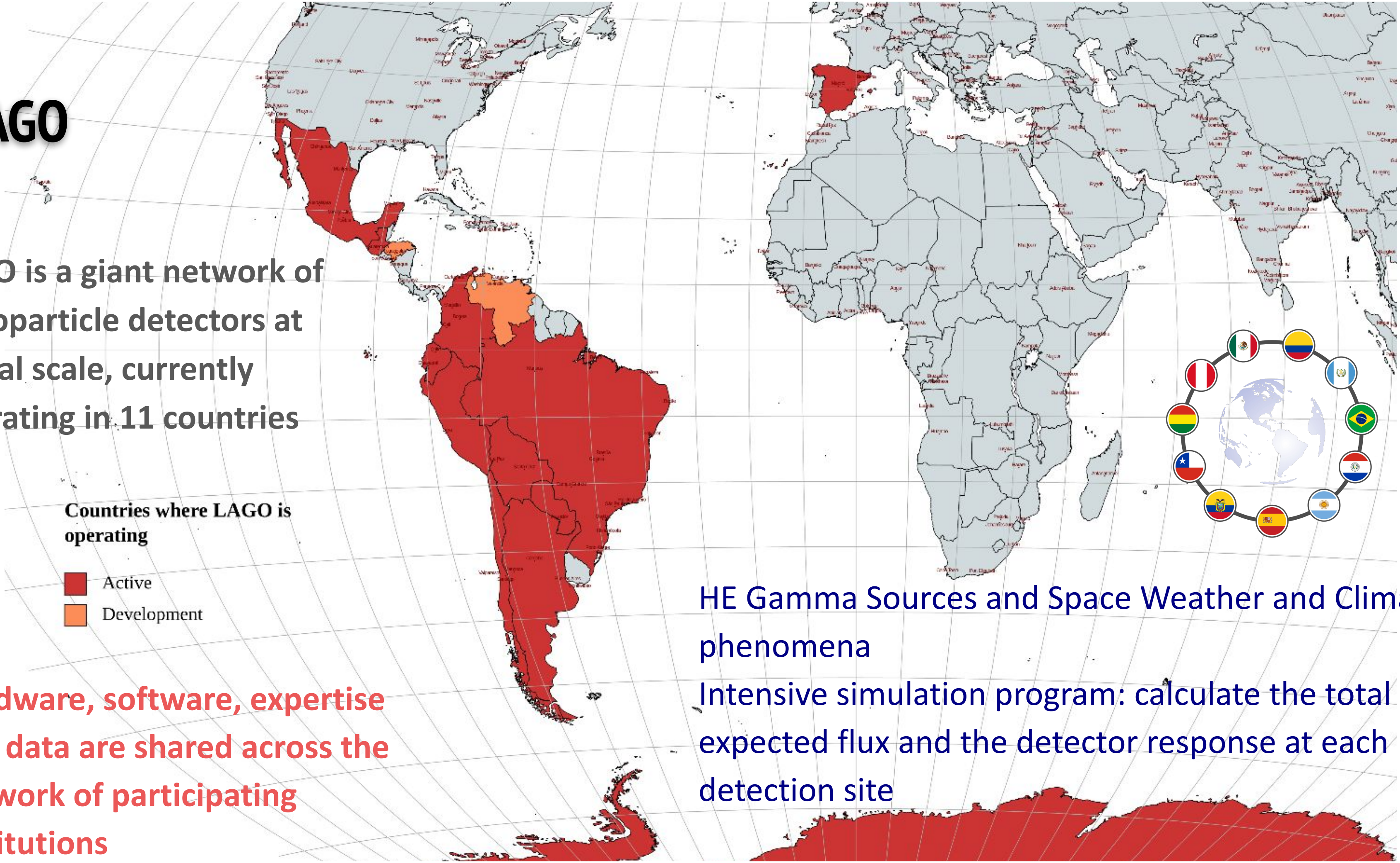

HE Gamma Sources and Space Weather and Climate phenomena

Intensive simulation program: calculate the total expected flux and the detector response at each detection site

Hardware, software, expertise and data are shared across the network of participating institutions

The Latin American Giant Observatory (LAGO)

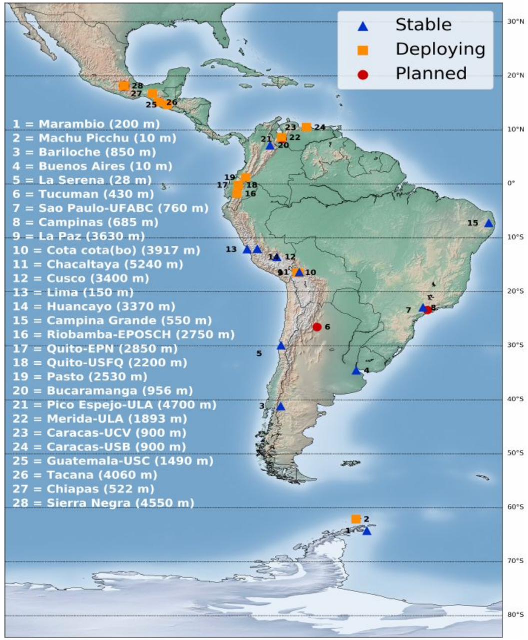

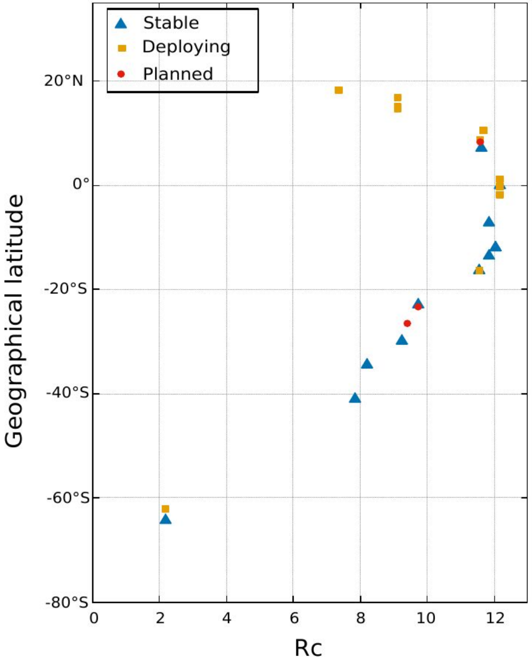

- Astroparticle physics to study the extreme universe
- Transient and long term space weather phenomena trough Solar modulation of Cosmic Rays
- Measurement of background radiation at ground level
- Academic goals
  - HEP and astro-ph seedbed for Ibero american students
  - Build an Ibero-American network of astroparticle researchers

[1] http://lagoproject.net/

Our detector: sWCD (Water Cherenkov Detector)

s as in *smart*

US$ ~9500

- Autonomous, reliable, simple and cheap detector
- Commercial tanks with $1{,}5\,\mathrm{m}^2 - 10\,\mathrm{m}^2$ of detection area filled with purified water
- Inner coating of Tyvek (UV diffusive and reflective fabric)
- PMT + Digitizer board (own design)
- FPGA + Raspberry Pi: detector control, telemetry, data acquisition and on board data pre-analysis (including machine learning techniques)

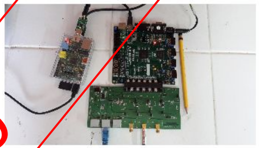

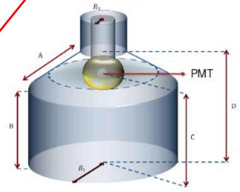

- Digitized signals by a 10-14 bits FADC at 40-100 MHz (10-25 ns)
- Temporal synchronization: GPS in PPS mode
- Station consumption: $\lesssim 8\,\mathrm{W}$

Implementing cost-effective instrumentation in order to have a decentralized and sustainable funding model.

LAGO

LAGO Space Weather Station (planned)

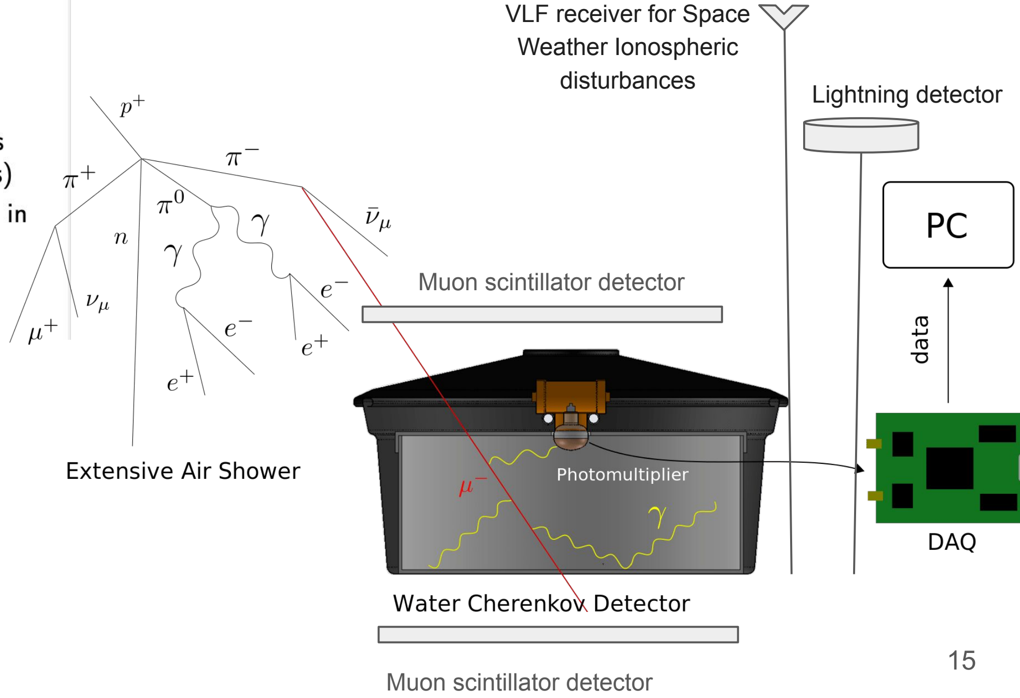

LAGO Capabilities: Multi-spectral analysis

- Simultaneous measurements of secondaries at ground level
- Intensive simulation and data analysis frameworks

Connections

$$\textbf{CR Flux} \xrightarrow{\text{Astrophysics transients}} \text{Modulated flux} \cdots$$

$$\cdots \text{Modulated flux} \xrightarrow{\text{Geomagnetic field}} \text{Primaries} \cdots$$

$$\cdots \text{Primaries} \xrightarrow{\text{Atmospheric conditions}} \text{Secondary particles} \cdots$$

$$\cdots \text{Secondary particles} \xrightarrow{\text{Detector response}} \textbf{Signals}$$

Synergy

Flux variation of signals at detector level⇔Transients

H. Asorey et al., PoS ICRC2015 142, 2015

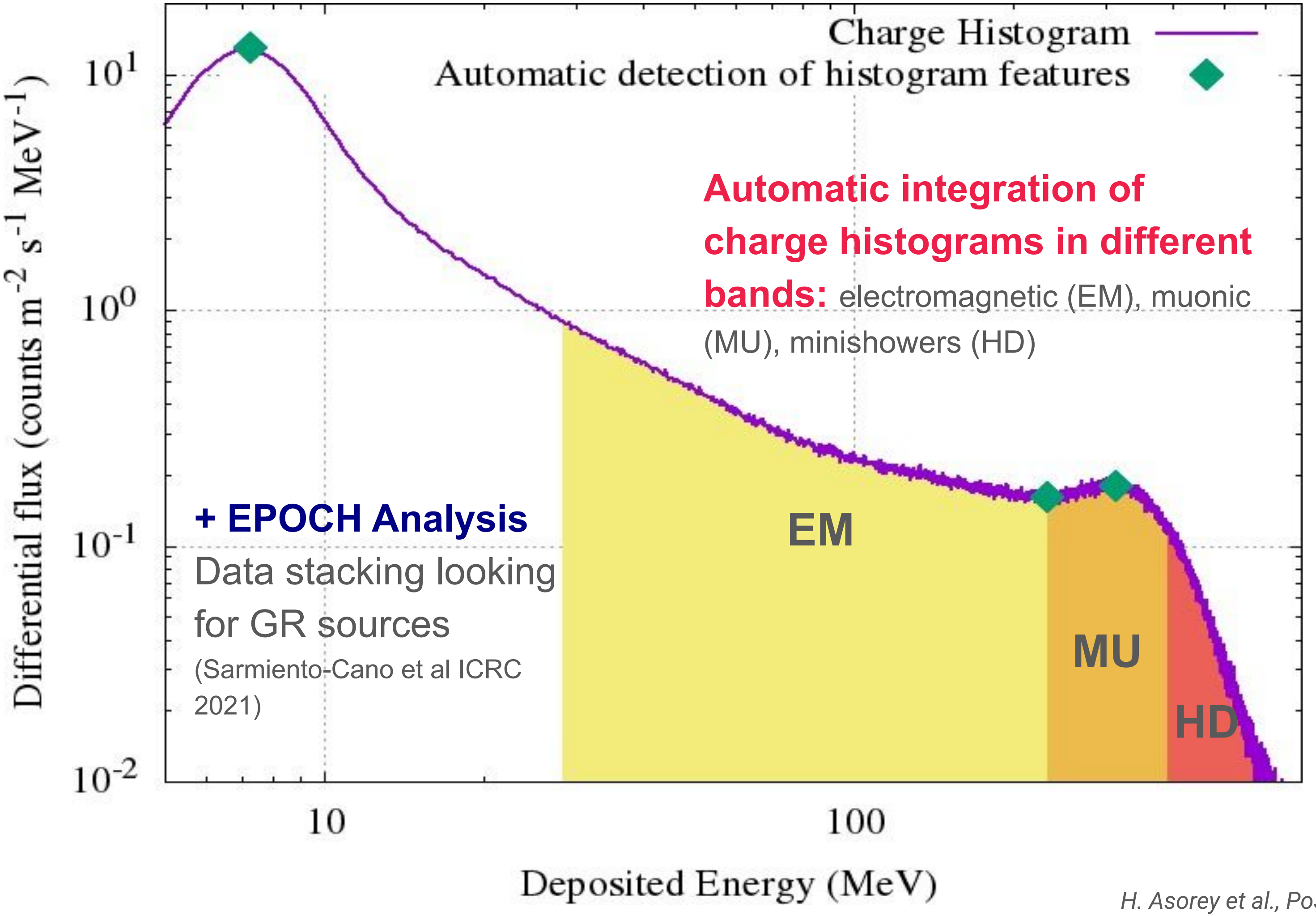

H. Asorey et al., PoS ICRC2015 142, 2015


clima espacial extremo


meteorología espacial extrema

Earth magnetic field

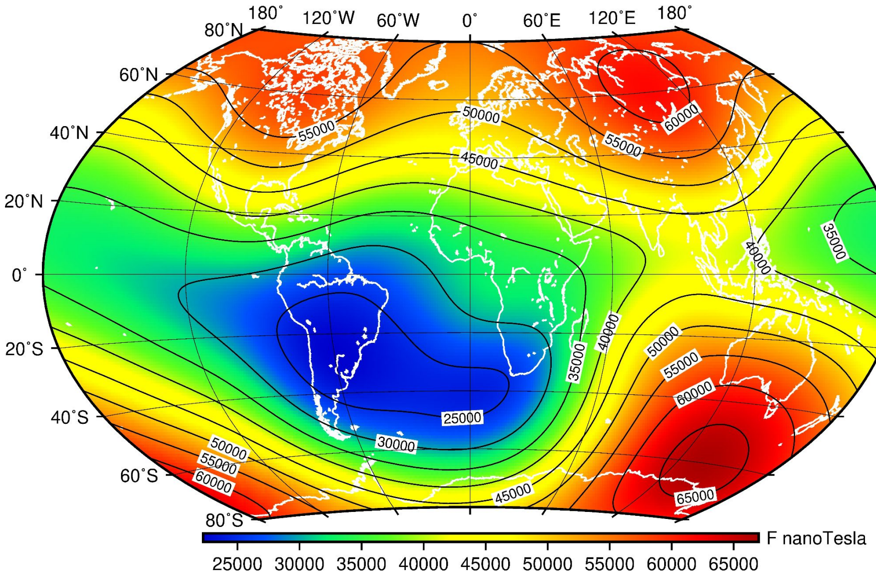

IGRF-13 Geomagnetic model (2020-24)

Total intensity flux for Jan'20

Multipole expansion up to l=13

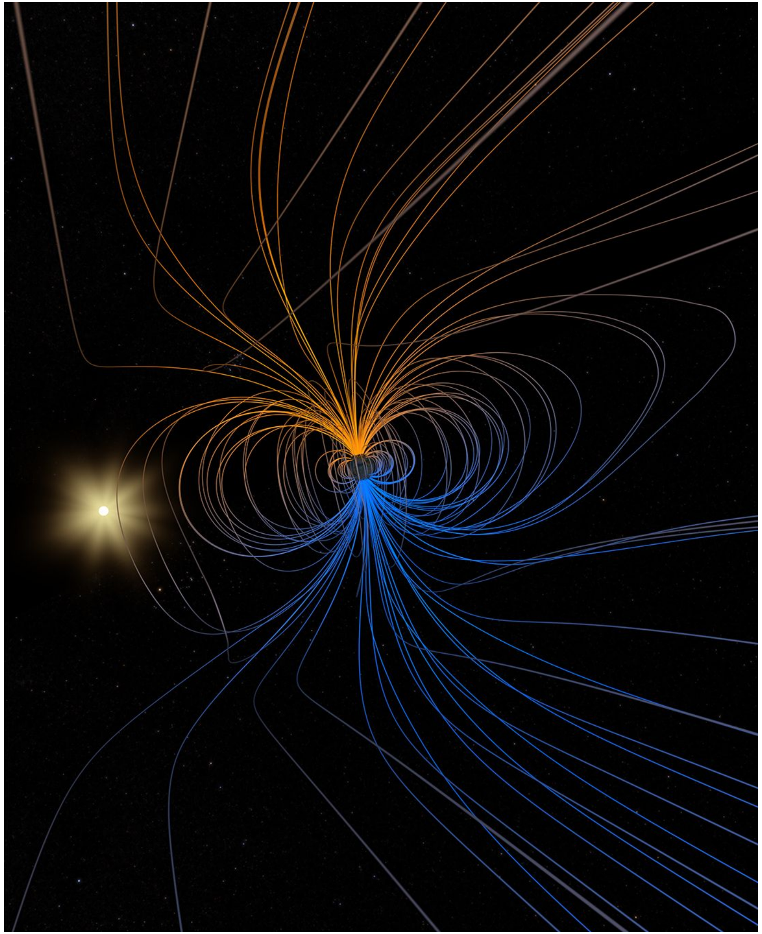

Solar wind effect, Tsyganenko model

Time-dependent local geomagnetic effects

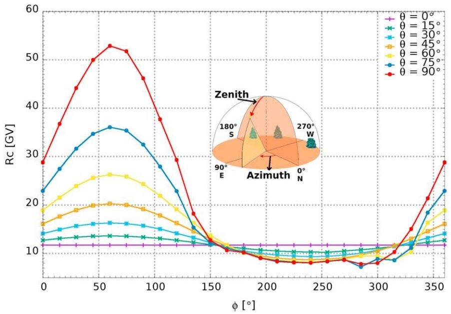

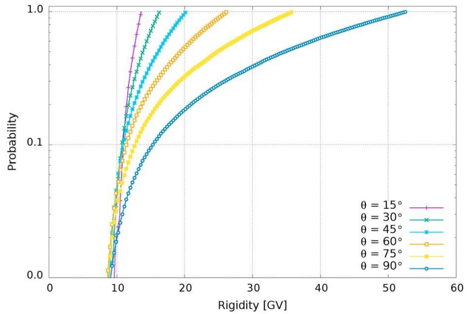

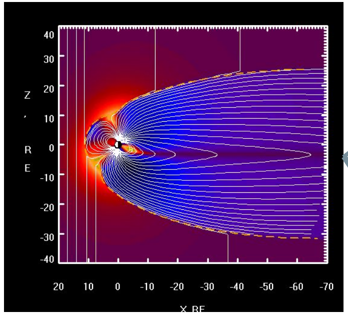

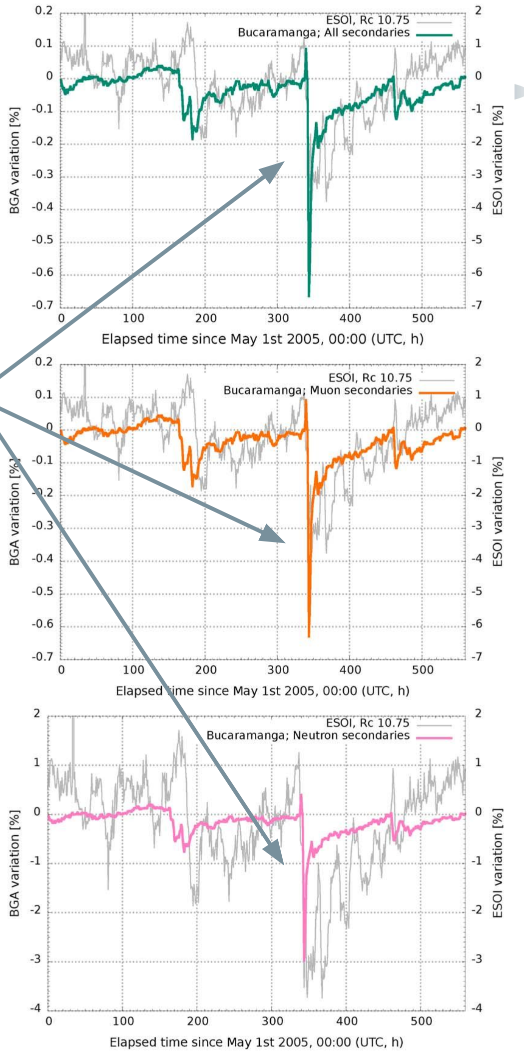

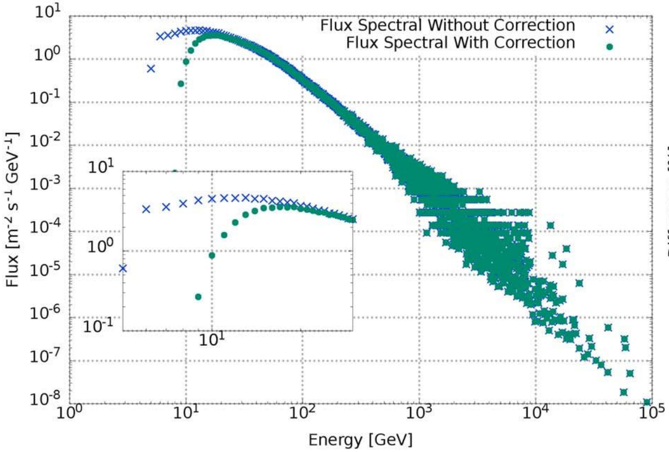

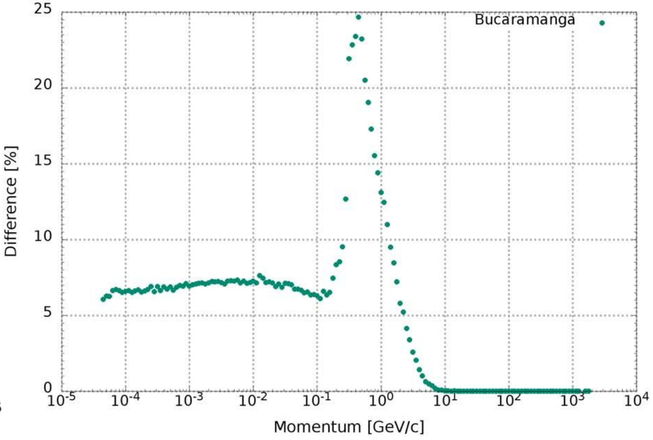

M. Suárez-Durán, H. Asorey and LA Núñez, Space Weather, (2018), [DOI:10.1002/2017SW001774](https://doi.org/10.1002/2017SW001774)

Extensive Air Showers (EAS): each cosmic ray interacts with the atmosphere producing a cascade of up to $>10^{10}$ secondary particles

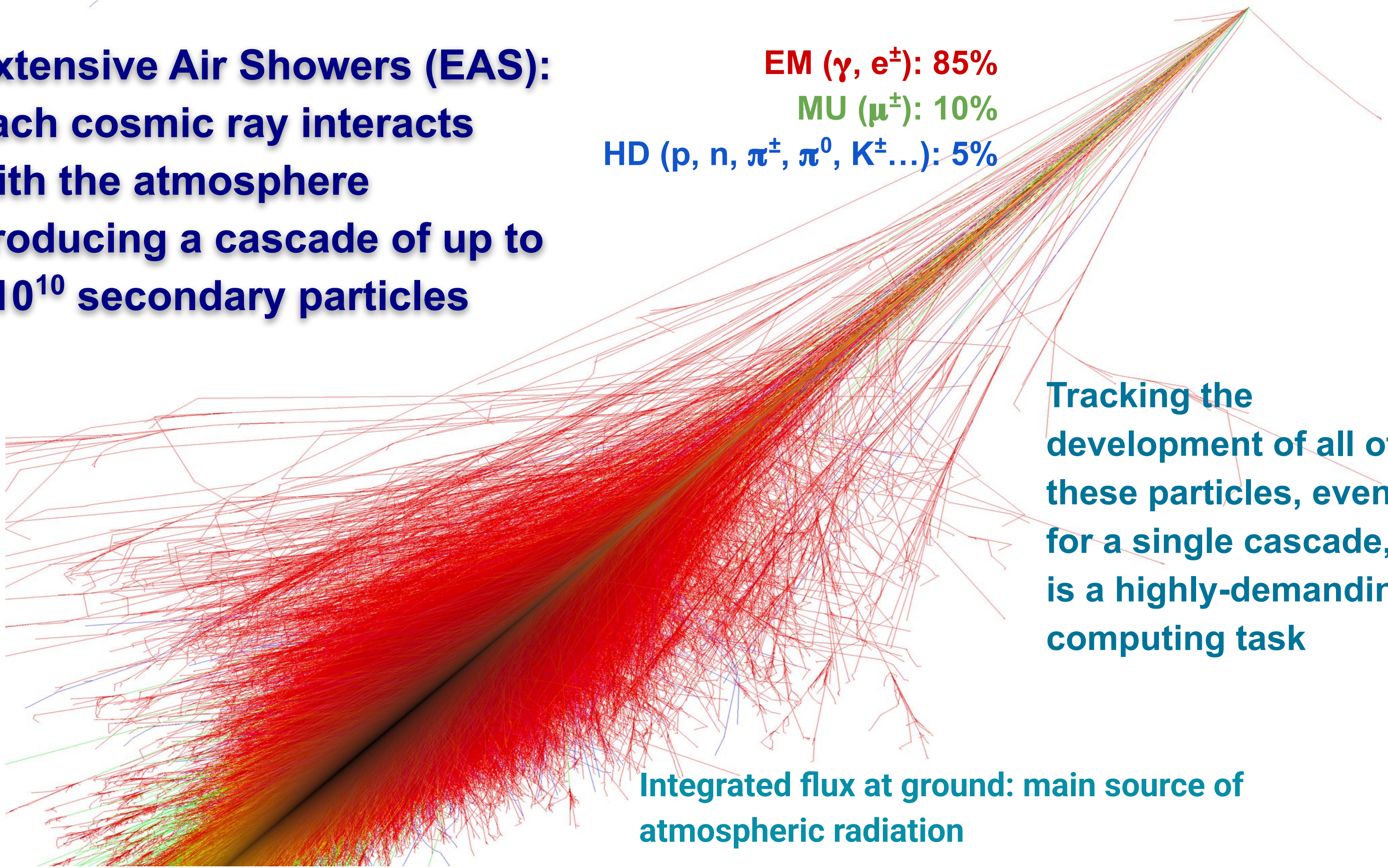

EM (γ, $e^{\pm}$): 85%

MU ($\mu^{\pm}$): 10%

HD (p, n, $\pi^{\pm}$, π^{0}, $K^{\pm}$…): 5%

Tracking the development of all of these particles, even for a single cascade, is a highly-demanding computing task

Integrated flux at ground: main source of atmospheric radiation

Our framework: integrated ARTI, CORSIKA & GEANT4

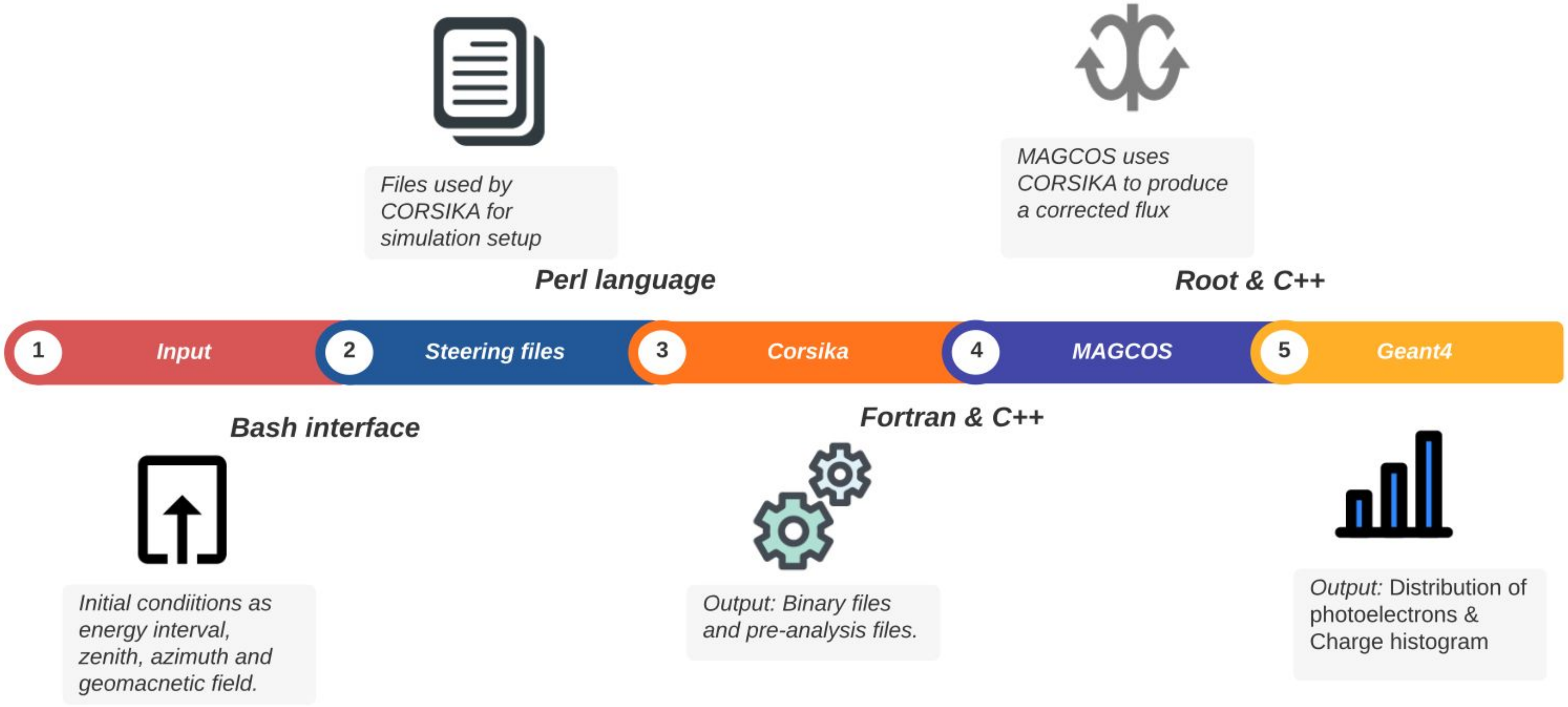

FAIR: los catálogos son encontrables, accesibles, interoperables y reusables

100k vuelos/día: mientras hablamos hay 7k aviones en el aire

Atmospheric reaction to CR is the main source of background radiation (plus natural radioactivity)

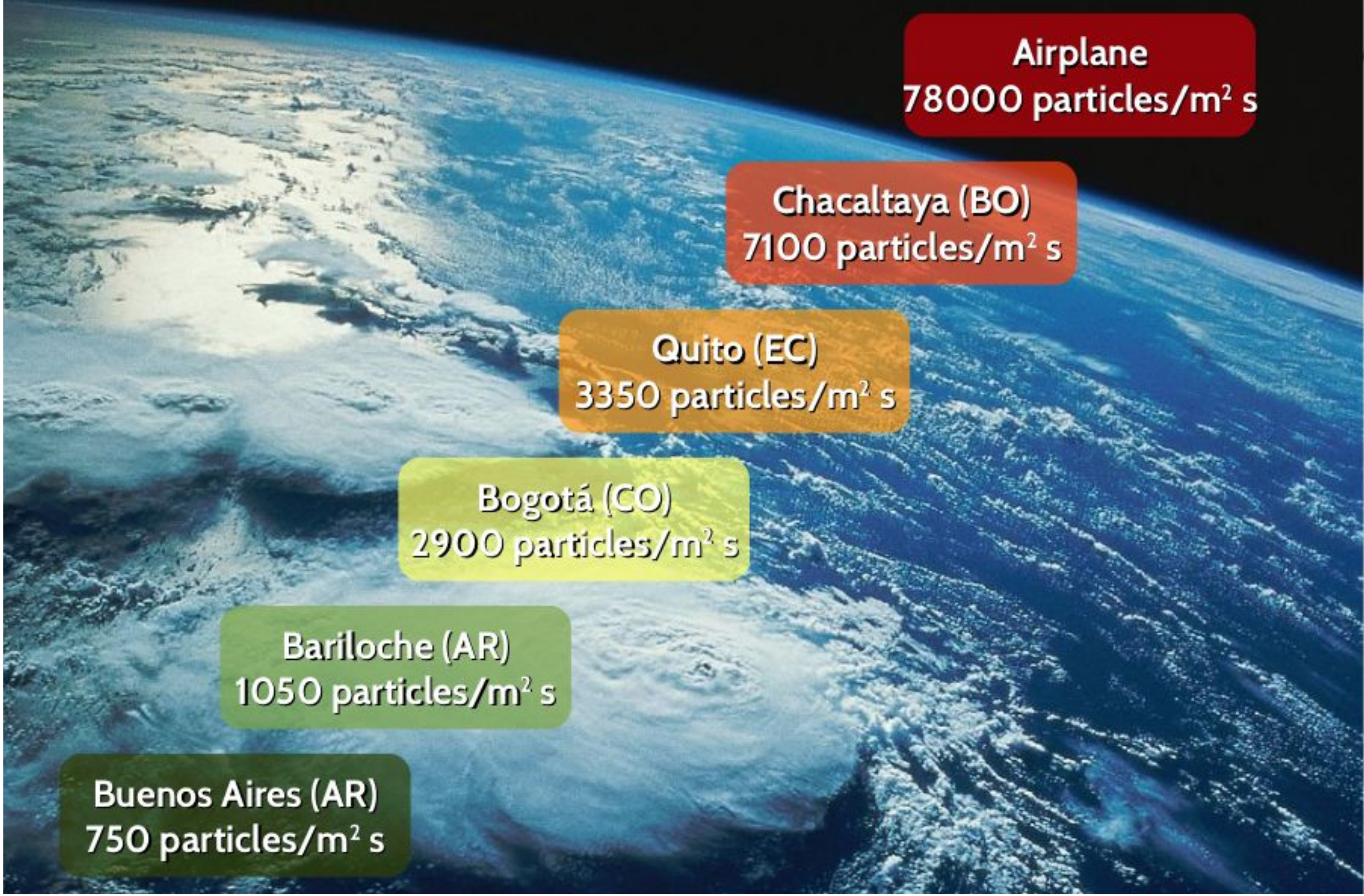

ACORDE: Application COde for the Radiation Dose Estimation

A tool designed to accurately calculate the radiation dose during commercial flights based on start-of-the-art codes

1. Segmentation of real flight paths from public databases

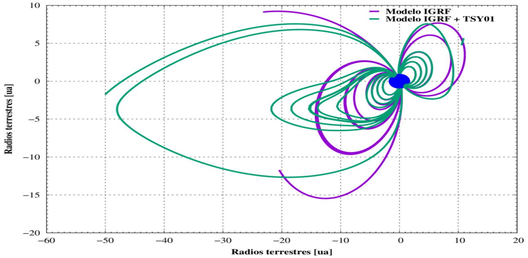

2. On route real-time EMF condition (IGRF13+TSY01

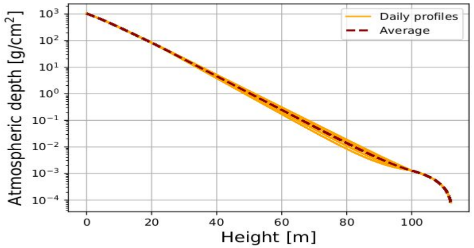

3. On route GDAS atmospheric profiles

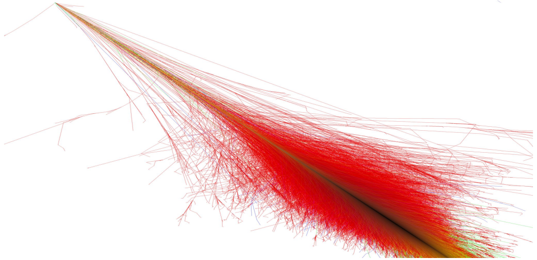

4. On route integrated secondary particles flux at flight altitude (ARTI)

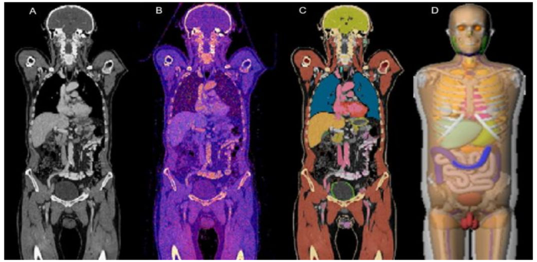

5. Dose calculation in Geant4 models of the aircraft and a human phantom

Asorey et al, JARI 2023

ACORDE calculation example: IB3270 MAD-HAM 6/Nov/2021

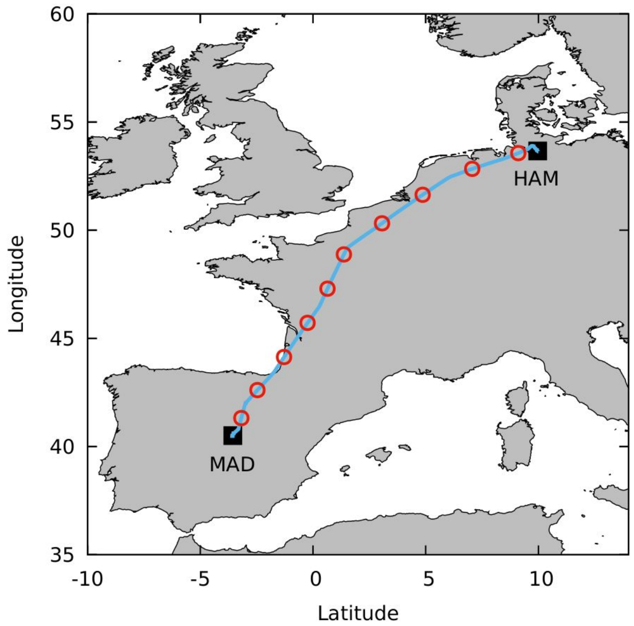

From the real track gathered from public databases, ACORDE segments the route and find the main waypoints

the worst case scenario is considered for mixed altitude segments

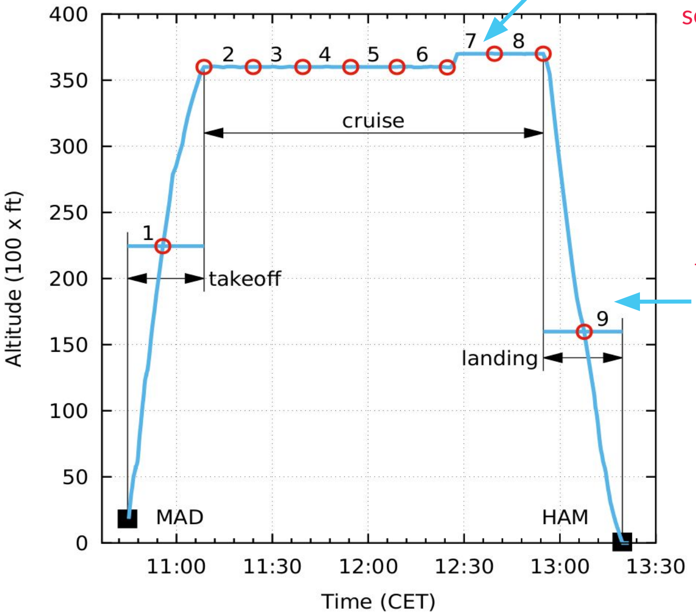

takeoff and landing waypoints are located at the midpoint of each interval

The cruise stage is automatically derived from the analysis of the track altitude as a function of time and its derivatives

Local GDAS atmospheric profiles at each waypoint

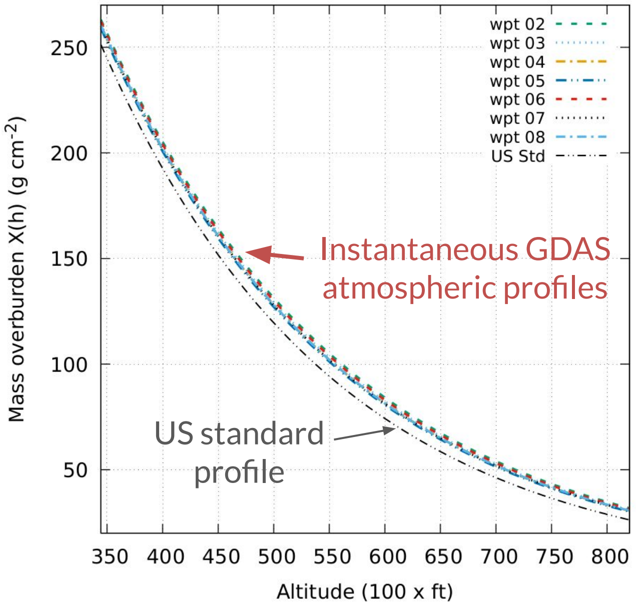

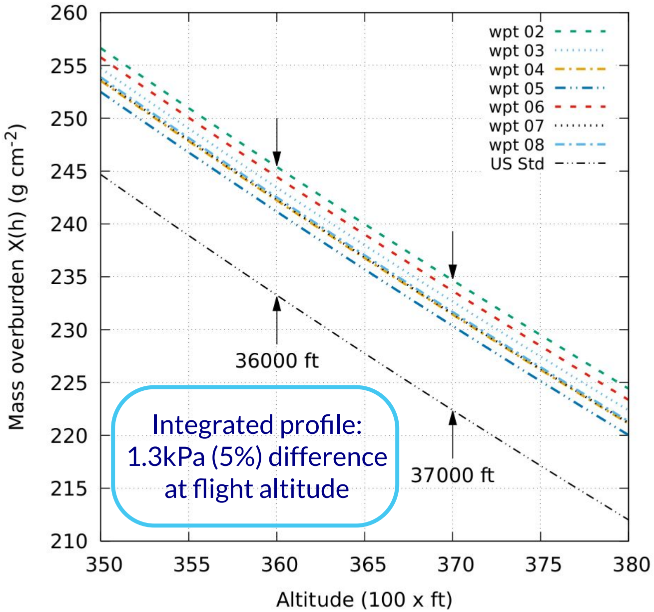

Atmospheric profiles are gathered from GDAS database for each waypoint within a ±1.5h time window and used for the corresponding segment

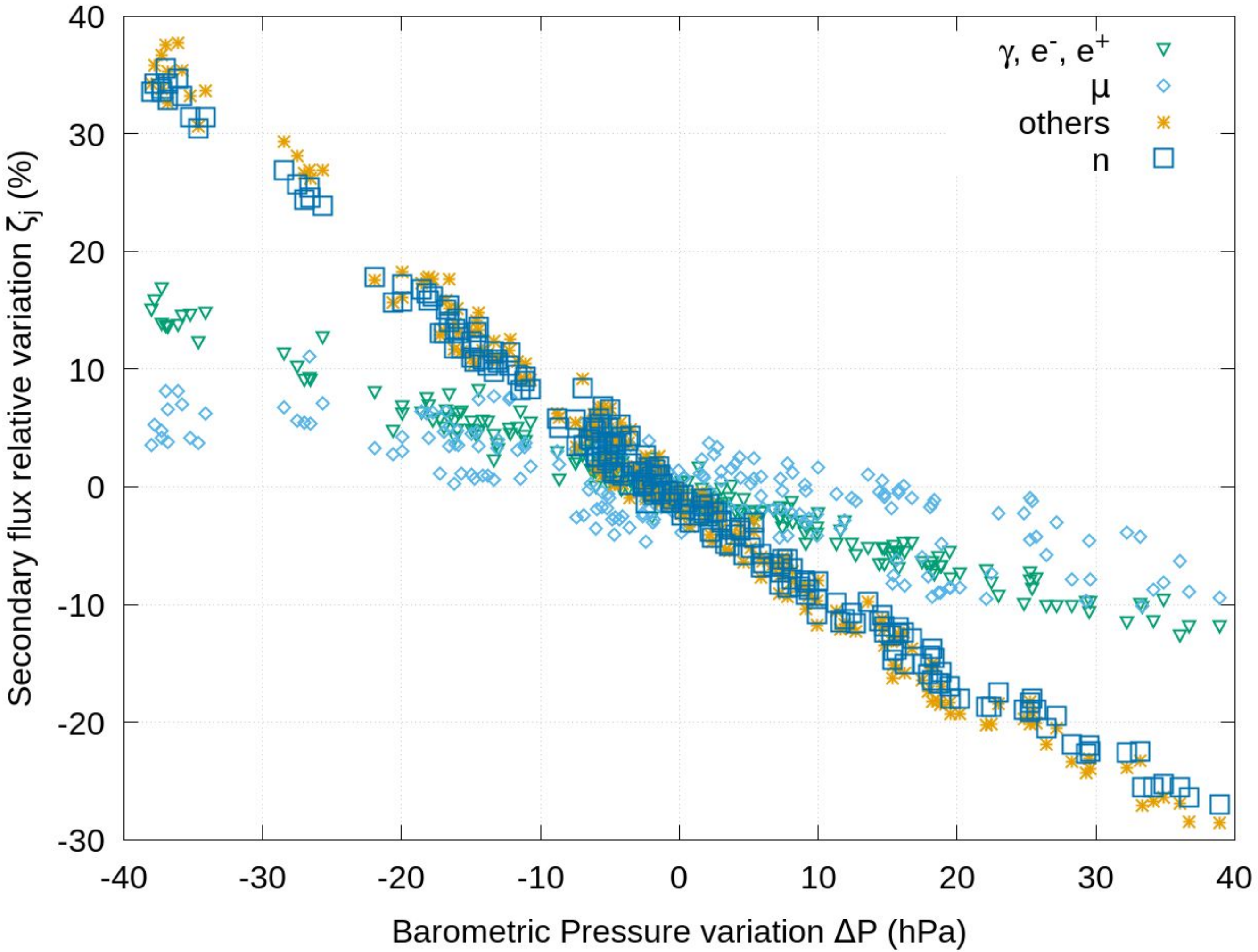

H. Asorey and R. Mayo-García, J. Supercomputing 2022, https://doi.org/10.1007/s11227-022-04981-8

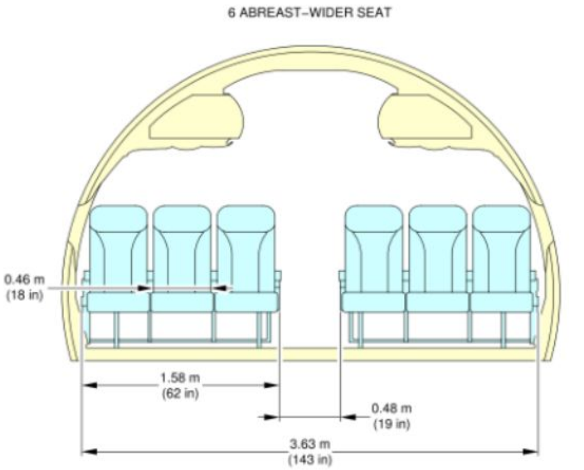

Vuelos comerciales
y
ciencia básica

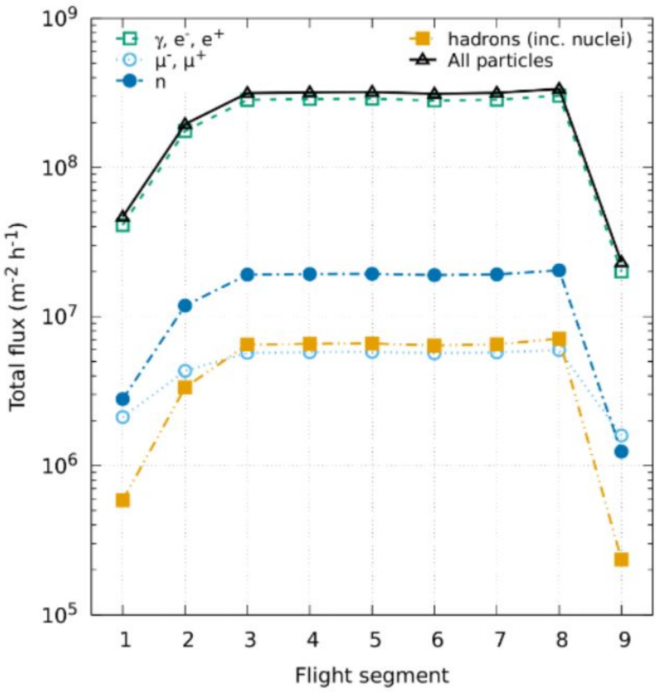

Modelo computacional (3D)

- Fuselaje
- Fantoma antropomórfico

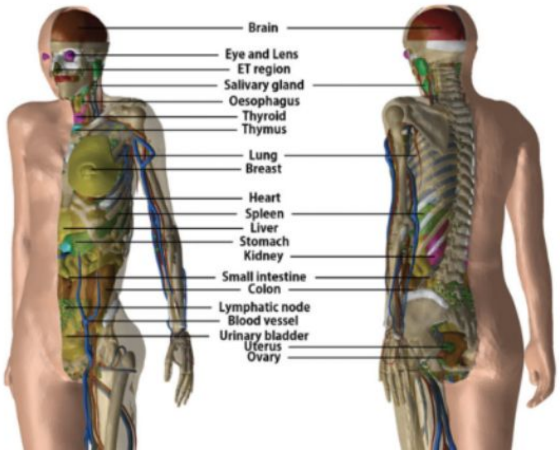

Extended simulation campaign: 324 flights

- 287 regular random IB flights
- 37 West-East and East-West flights operated by JL and CX
- ACORDE dose (E_A) compared with CARI-7A standard calculation dose (E_C)
- Absolute

$$\Delta E = (E_A - E_C)$$

and relative differences

$$\Delta E_{\%} = 2\,\Delta E / (E_A + E_C)$$

were computed and averaged

- **long flights: significant differences**

1: Short (153), 2: Intermediate (58), 3: Long (113), $3^{\dagger}$: Regular flights (76), $3^{\ddagger}$: W-E and E-W flights (37)

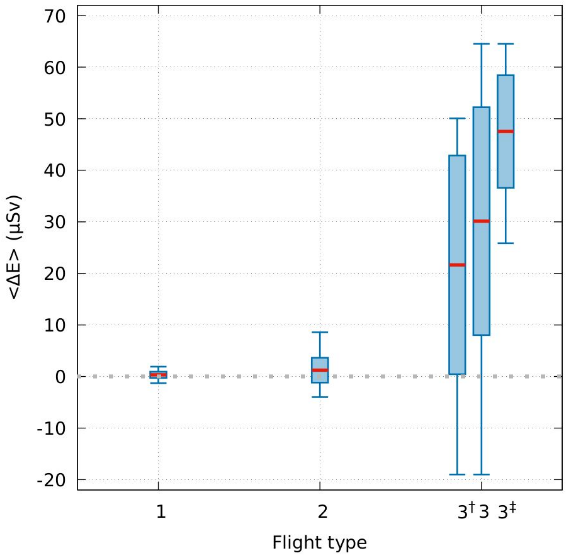

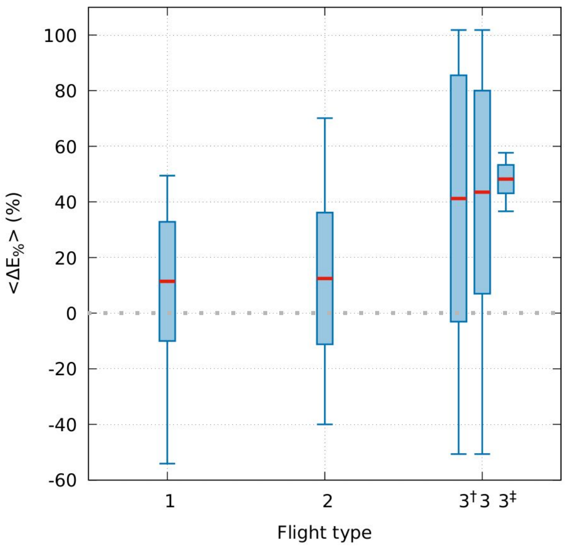

Type 3	$\langle \Delta E \rangle = (30 \pm 22)$ μSv	$\langle \Delta E_{\%} \rangle = (44 \pm 37)$ %
Type $3^{\dagger}$	$\langle \Delta E \rangle = (22 \pm 21)$ μSv	$\langle \Delta E_{\%} \rangle = (41 \pm 44)$ %
Type $3^{\ddagger}$	$\langle \Delta E \rangle = (48 \pm 11)$ μSv	$\langle \Delta E_{\%} \rangle = (48 \pm 5)$ %

GCR Flux → Heliosphere → **Modulated Flux** → Magnetosphere → **Primaries** → Atmosphere → **Secondaries** → Detector → **Signals or Doses**

From Astroparticle to Applications

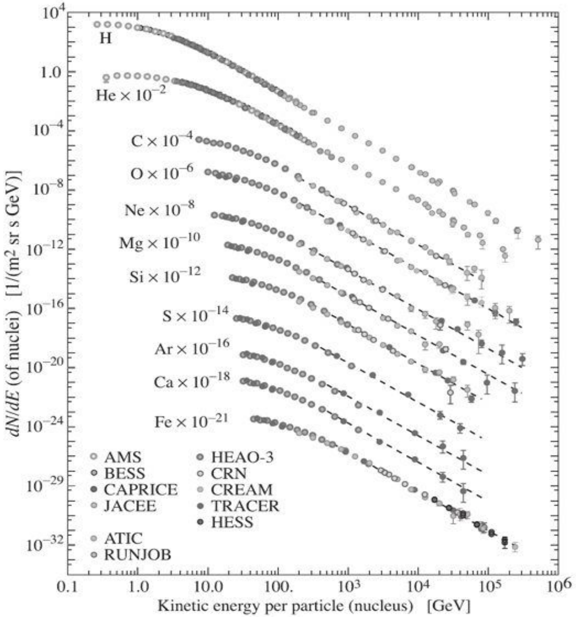

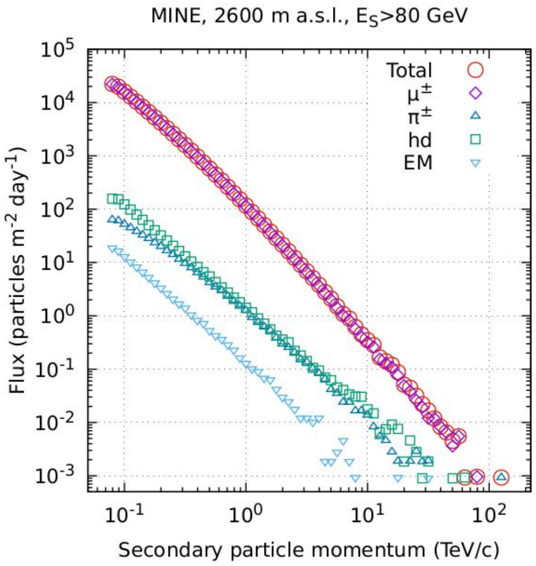

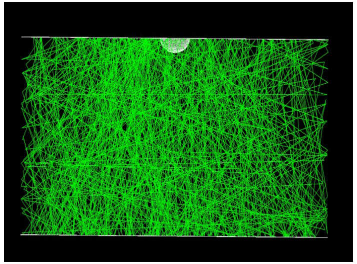

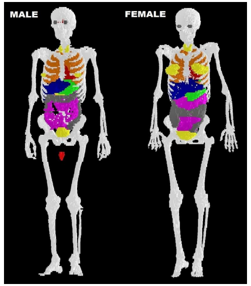

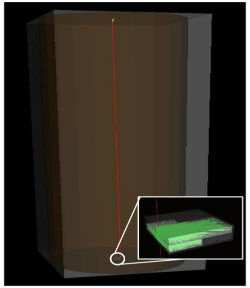

ARTI + CORSIKA **ARTI** **ARTI + MEIGA (Geant4)**

C. Sarmiento Cano et al., EPJ C in press, 2022, arXiv:2010.14591

Desarrollo de un “FAIRificador” universal para “open radiation”

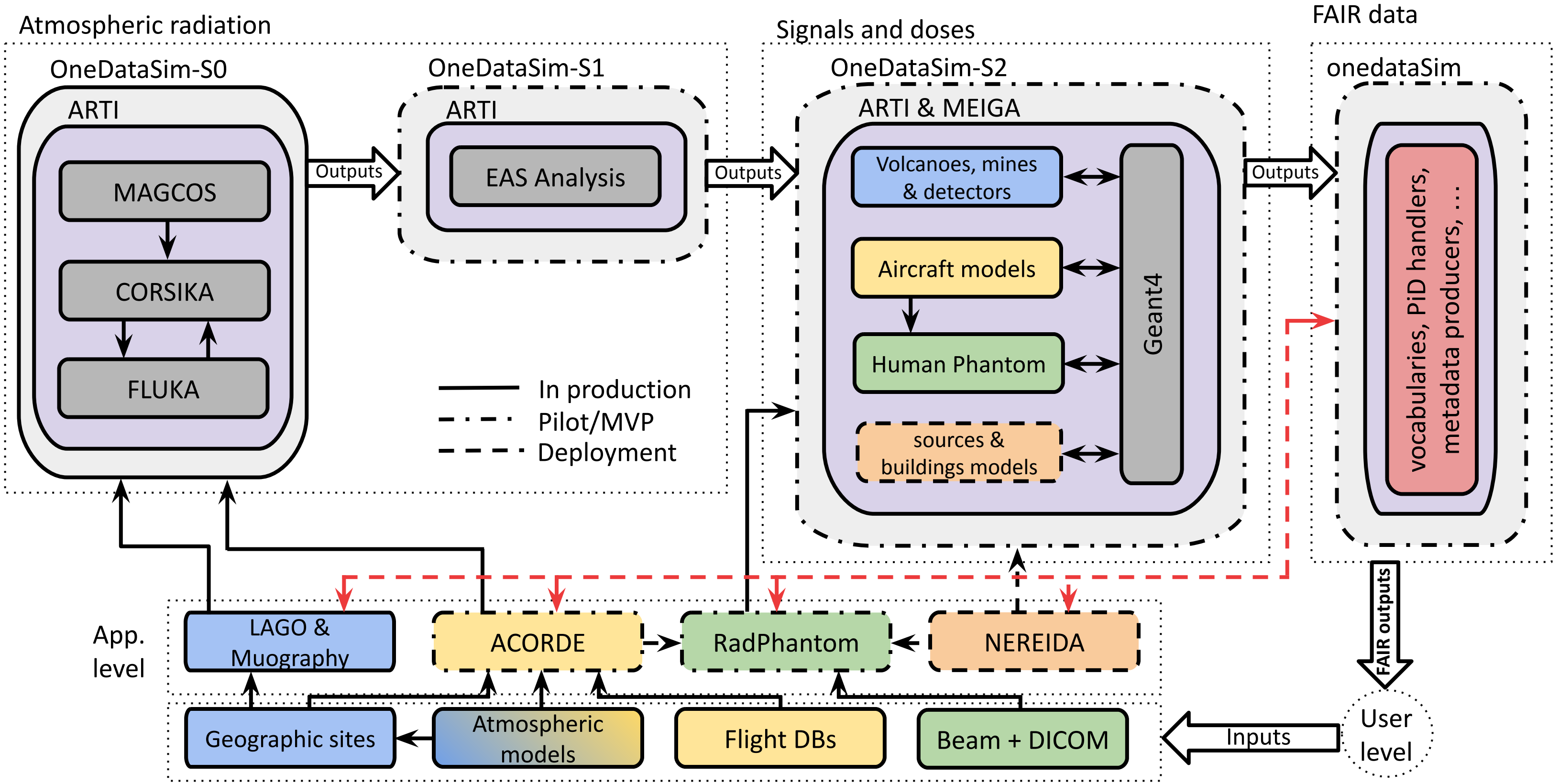

LAGO en la nube

Un proveedor de servicios HPC asigna recursos cloud a la EOSC:
n nodos, *r* GB/TB of RAM, *d* TB almacenamiento

Infrastructure Manager

Servicio basado en web con plantillas para distribuir recursos disponibles en clústeres virtuales. Instala el sistema operativo, en nuestro caso, Ubuntu 22.04 + gestor SLURM

docker HUB

contenedores docker con nuestros códigos se despliegan en el cluster virtual desde docker HUB

cluster virtual

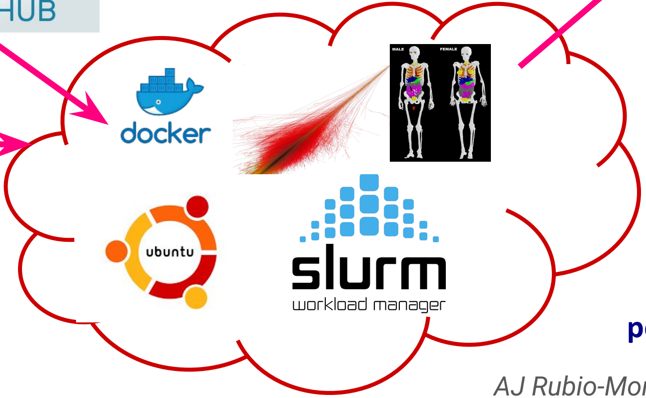

aws

Google Cloud

Microsoft Azure

B2FIND

FAIR: los catálogos son encontrables, accesibles, interoperables y reusables

ONEDATA

Los resultados se almacenan en un almacenamiento cloud accesible por tokens

B2HANDLE

se asignan PIDs (Identificadores persistentes) a cada catálogo de datos

AJ Rubio-Montero et al., IEEE WSC2021 21706697, 2021

Plataforma de gestión de grupos de investigación

MiLab
Ciencia abierta y reproducibilidad

- Plataforma como servicio en la nube para preservar la historia y facilitar la gestión de pequeños/medianos grupos de investigación (10-30):
  - Datos de investigación
  - Códigos informáticos
  - Entornos informáticos
  - Comunicación
  - Visibilidad web

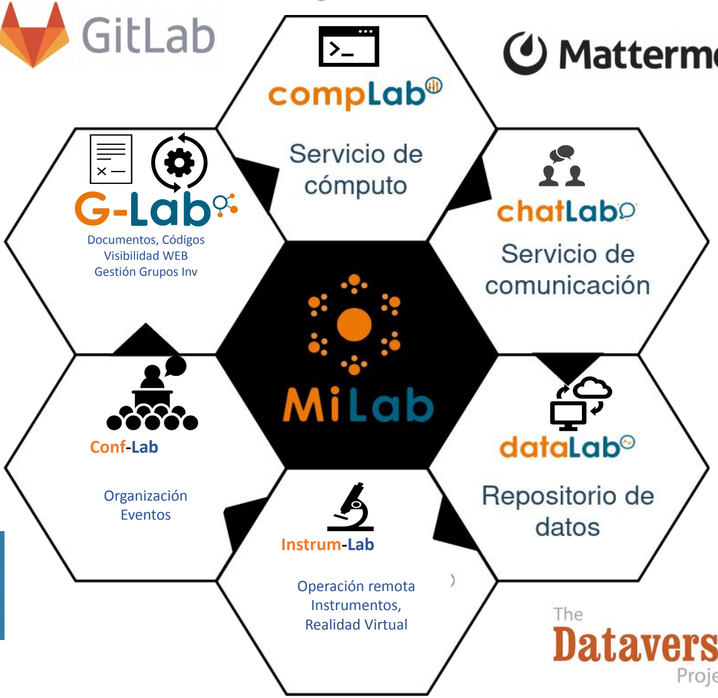

jupyter GitLab Mattermost zoom indico The Dataverse Project

cedia RedCLARA

Latin American alliance for Capacity buildiNG in Advanced physics
LA-CoNGA physics


geología extrema


Pyroclastic flows normally travel to distances of 5 to 10 kilometres
GVM

¿Cómo ver el interior de algo sin romperlo?


¿Cómo ver el interior de algo sin romperlo?

Los muones atmosféricos pueden atravesar hasta 2000 m de roca

Muography

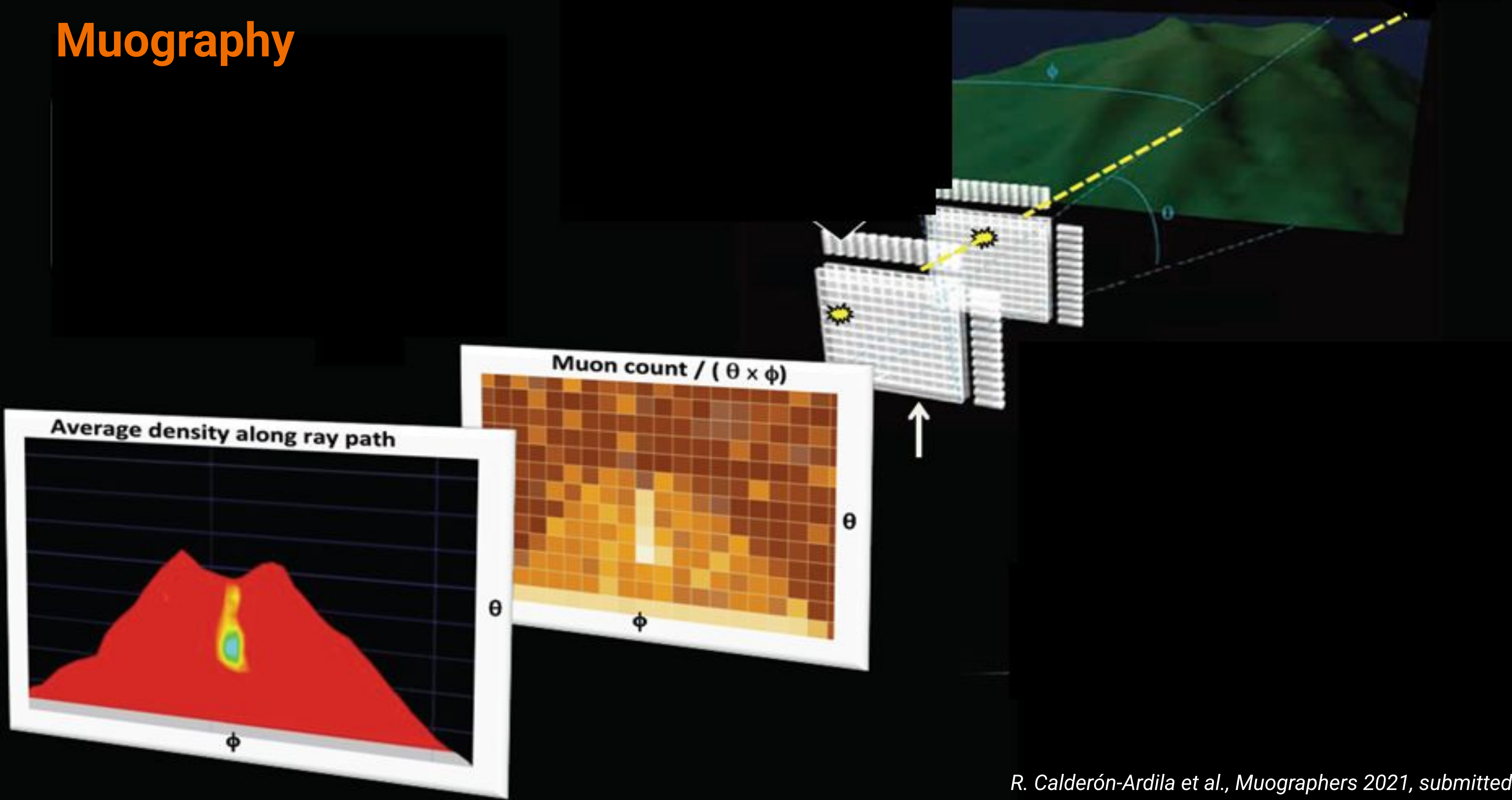

R. Calderón-Ardila et al., Muographers 2021, submitted

Muography, how to

- Start with an object with an unknown density profile
  - … measure the directional muon flux through this object
  - … and compare with the muon reference flux
  - → **you get the directional opacity of this object [g/cm²]**
- Additionally…
  - … obtain the external geometry of the object
  - → **and calculate the directional interaction distance [cm]**
- Finally, from…
  - directional opacity
  - directional interaction distances
- → **get internal density profile along muon propagation direction**

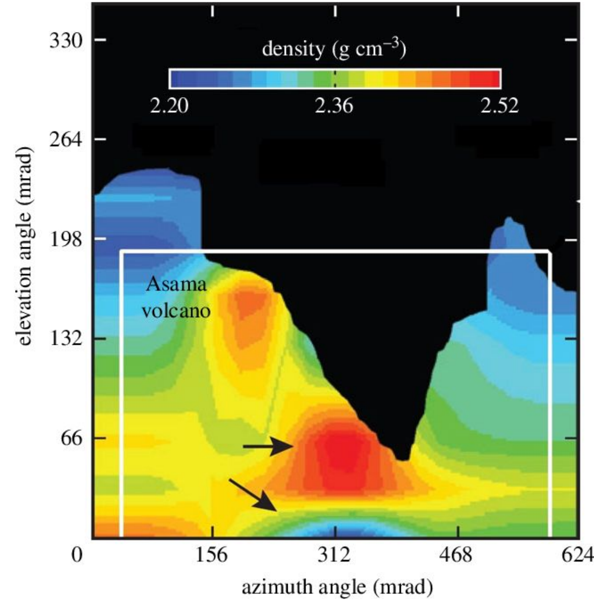

$$\boxed{\varrho(L)} \equiv \int_{\boxed{L}} \boxed{\rho(\xi)}\, d\xi\,,$$

MuTe 2.0 (2024)

Centelladores orgánicos en matriz plástica
y fibras ópticas centelladoras, SSD-Auger

Contadores Multipixel de Fotones en Silicio MPPC-SiPM

Detectores Extremos para Objetos Extremos
Centelladores, fibras y SiPM en MuTe (UIS)


Detectores Extremos para Objetos Extremos
Centelladores, fibras y SiPM en MuTe (UIS)

Electrónica desarrollada en UIS

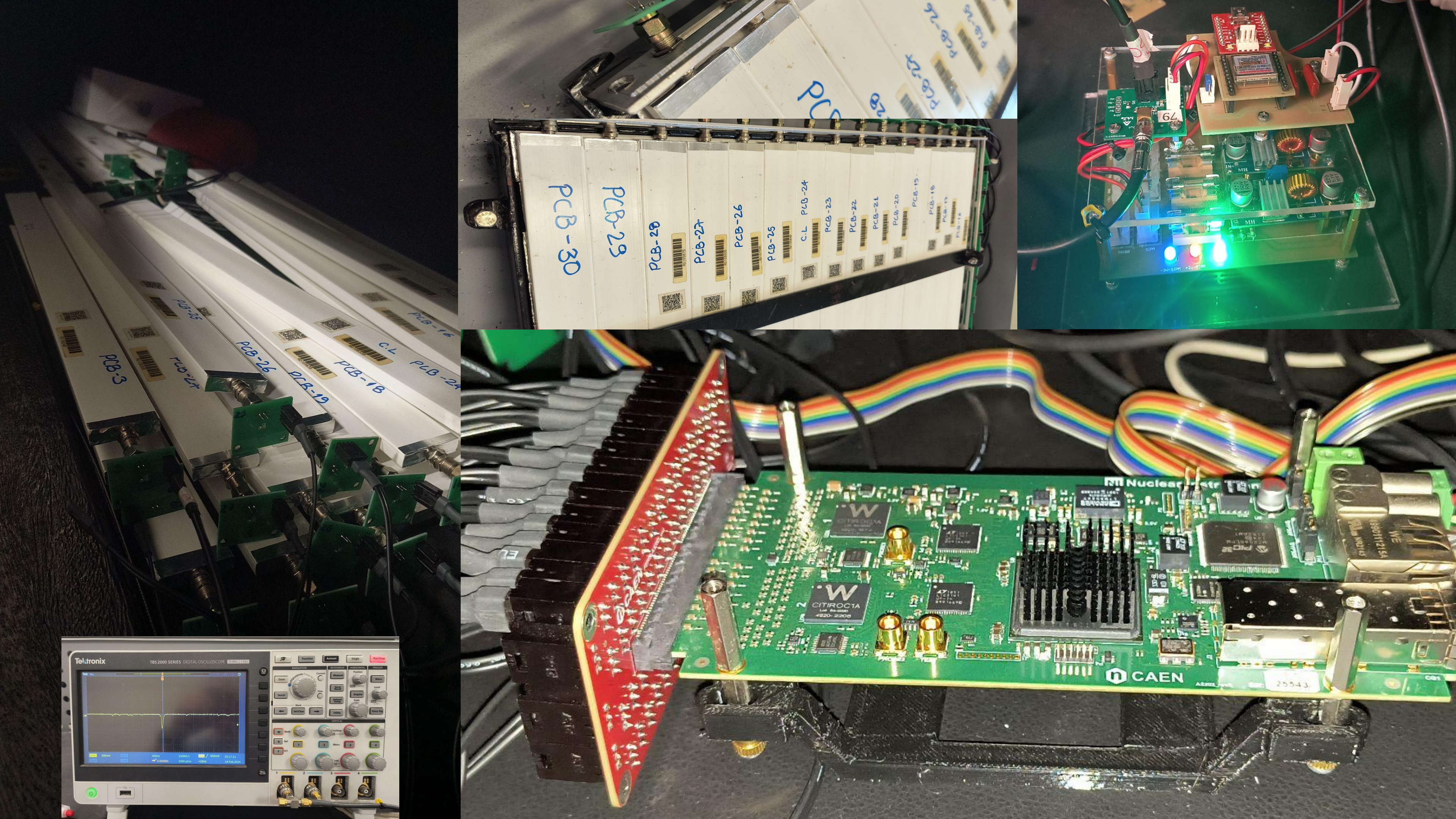

PCB-30
PCB-29
PCB-28
PCB-27
PCB-26
PCB-25
C.L
PCB-24
PCB-23
PCB-22
PCB-3
PCB-19
PCB-18
Tektronix
TBS 2000 SERIES DIGITAL OSCILLOSCOPE
CITIROC1A
CAEN

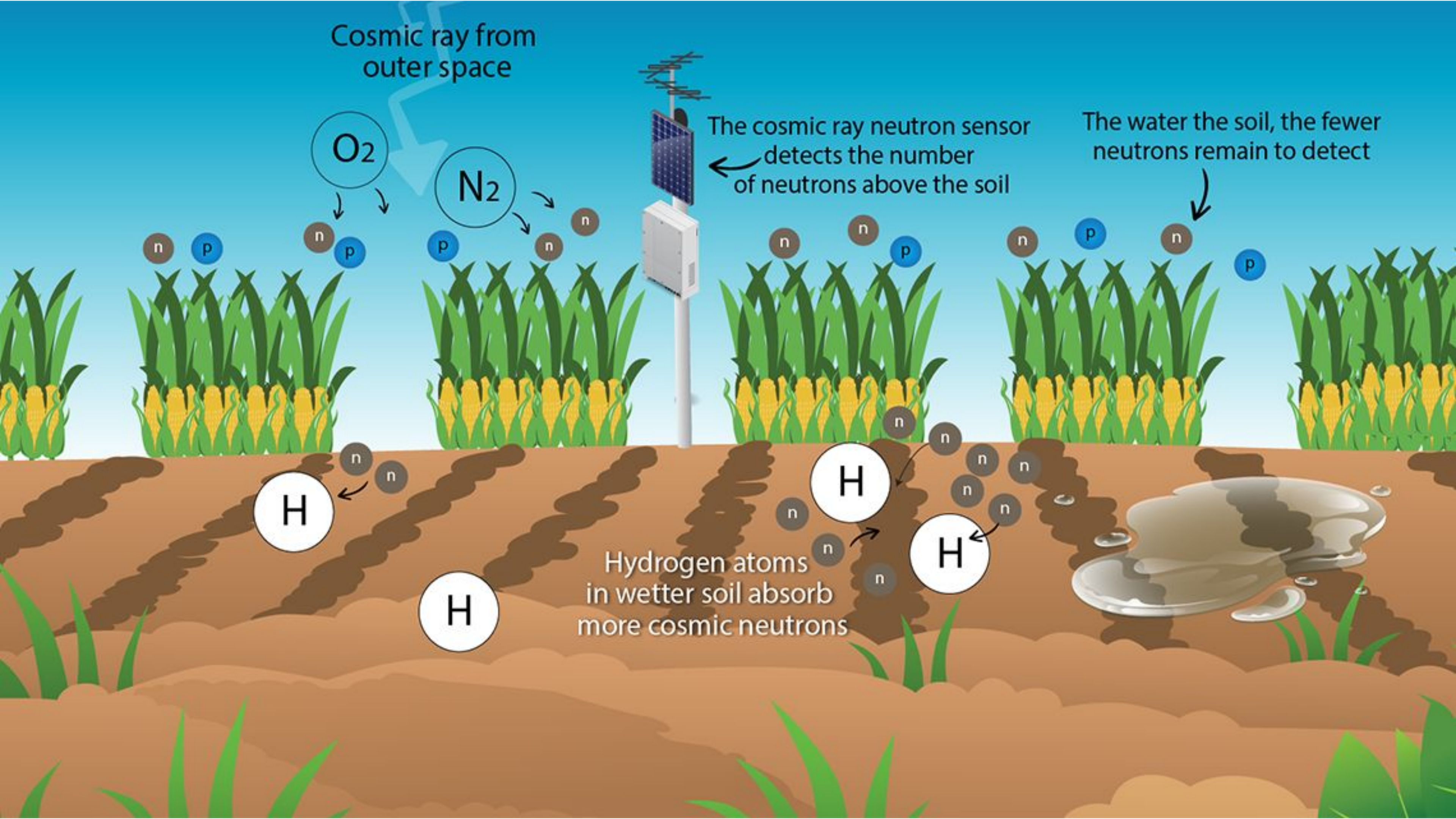

Cosmic ray from outer space
O_2
N_2
The cosmic ray neutron sensor detects the number of neutrons above the soil
The water the soil, the fewer neutrons remain to detect
n
p
H
Hydrogen atoms in wetter soil absorb more cosmic neutrons

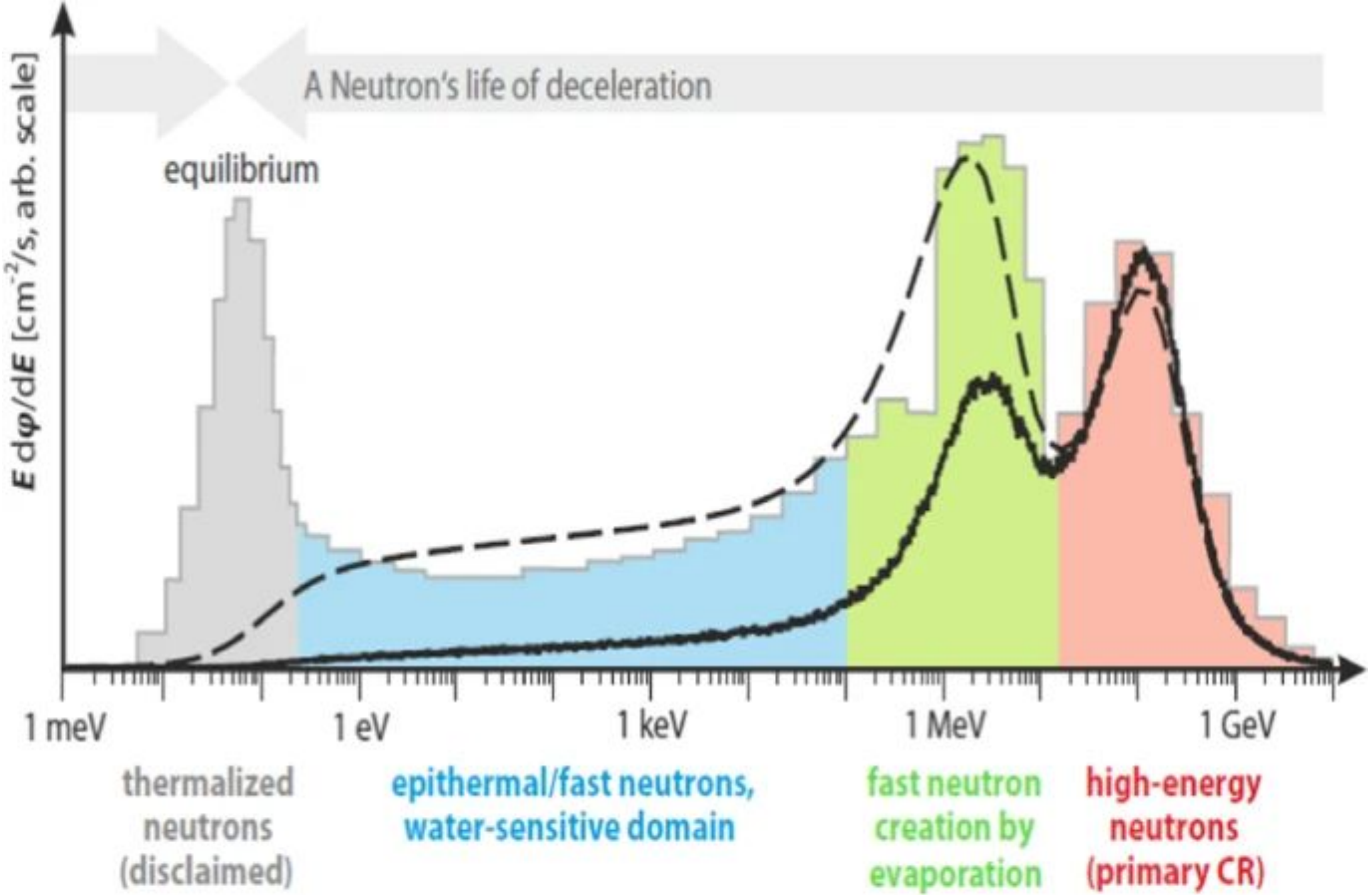
A Neutron's life of deceleration
equilibrium
E dφ/dE [cm⁻²/s, arb. scale]
1 meV
1 eV
1 keV
1 MeV
1 GeV
thermalized neutrons (disclaimed)
epithermal/fast neutrons, water-sensitive domain
fast neutron creation by evaporation
high-energy neutrons (primary CR)

¡Primeros resultados obtenidos para Bucaramanga!

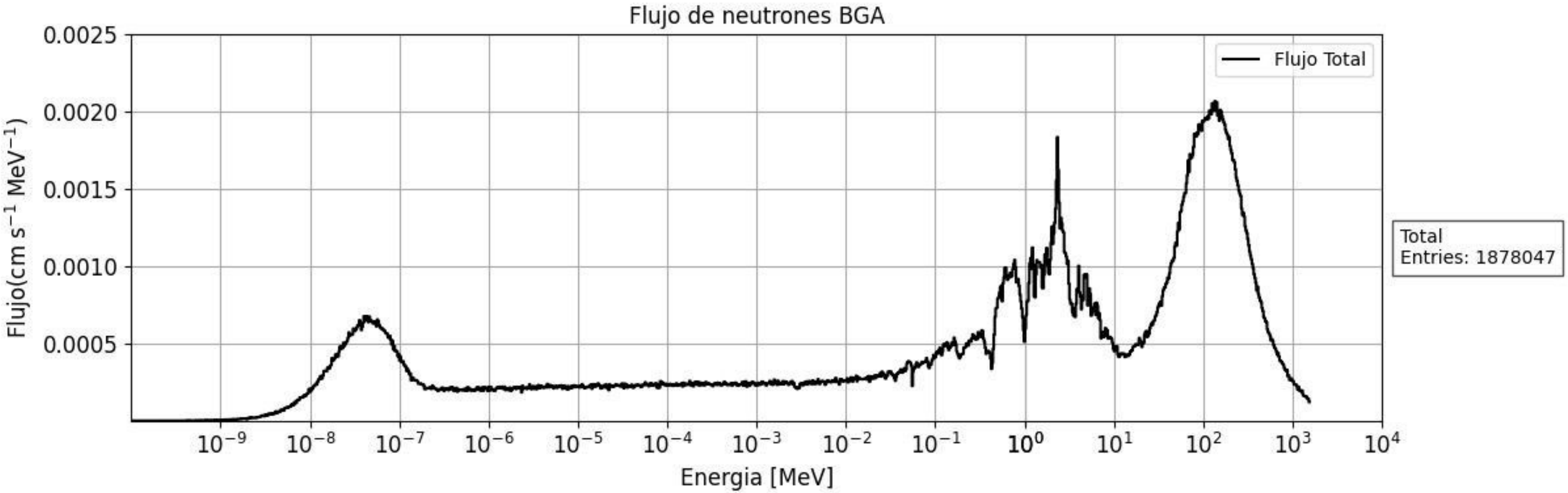

NEREIDA
NEutrones Rápidos para la Explotación de Instalaciones con Dispositivos Atómicos

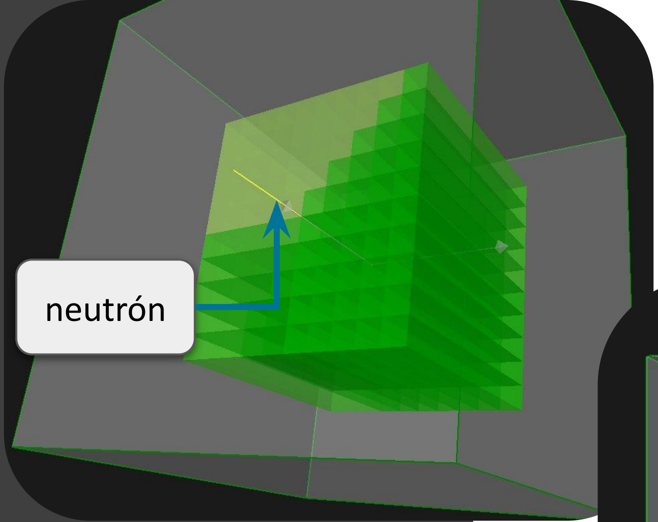

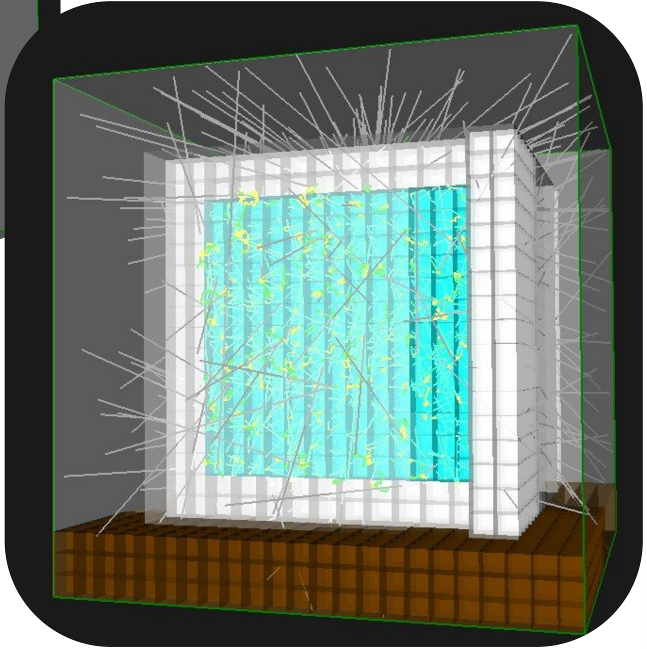

n p e^+ e^- γ $\bar{\nu}_e$

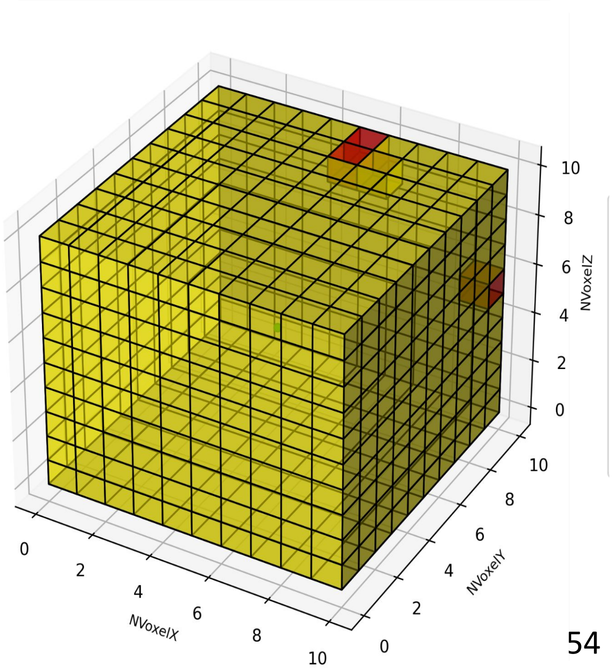

¿Podremos usar esta tecnología para diagnóstico o tratamiento?

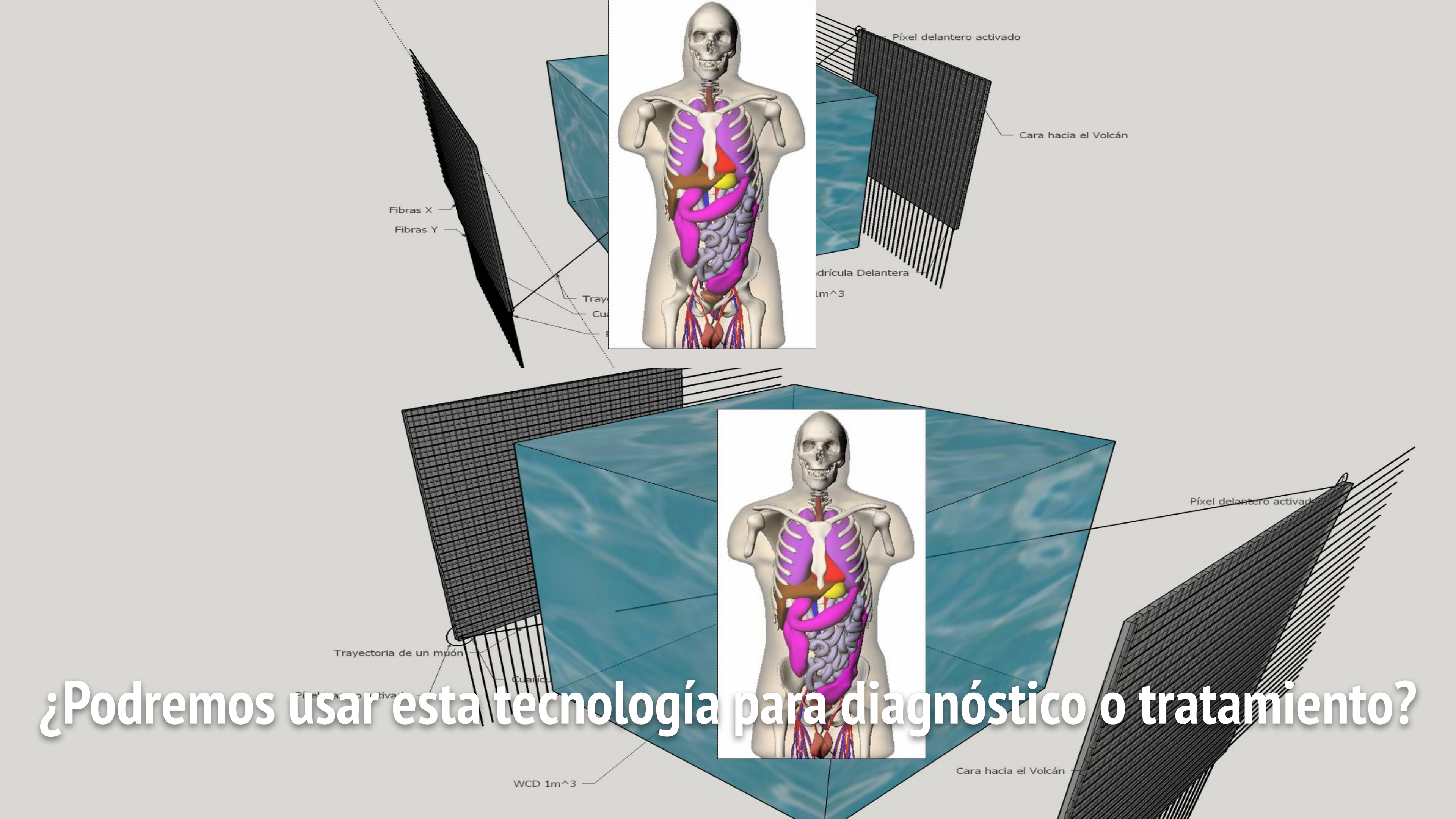

FAIRSFAIR
Fostering Fair Data Practices in Europe

New application: RadPhantom

Develop digital twin systems for calculating the effective dose in humans exposed to high doses of environmental radiation. In the simulation of these digital twins, Monte Carlo simulation techniques are applied for the implementation of a new MEIGA application in virtualized environments.

DICOM images from real patients

Voxelized ICRP110 phantom

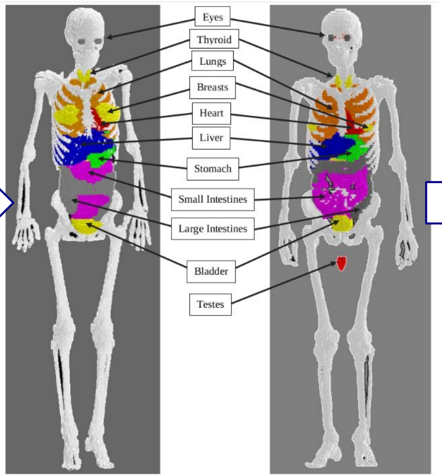

Geant-4 model

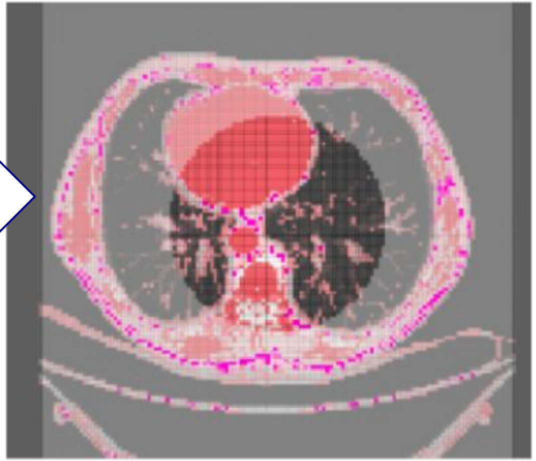

Large et al, 2020; Núñez-Chongo et al., IEEE 2023

3D dose deposition

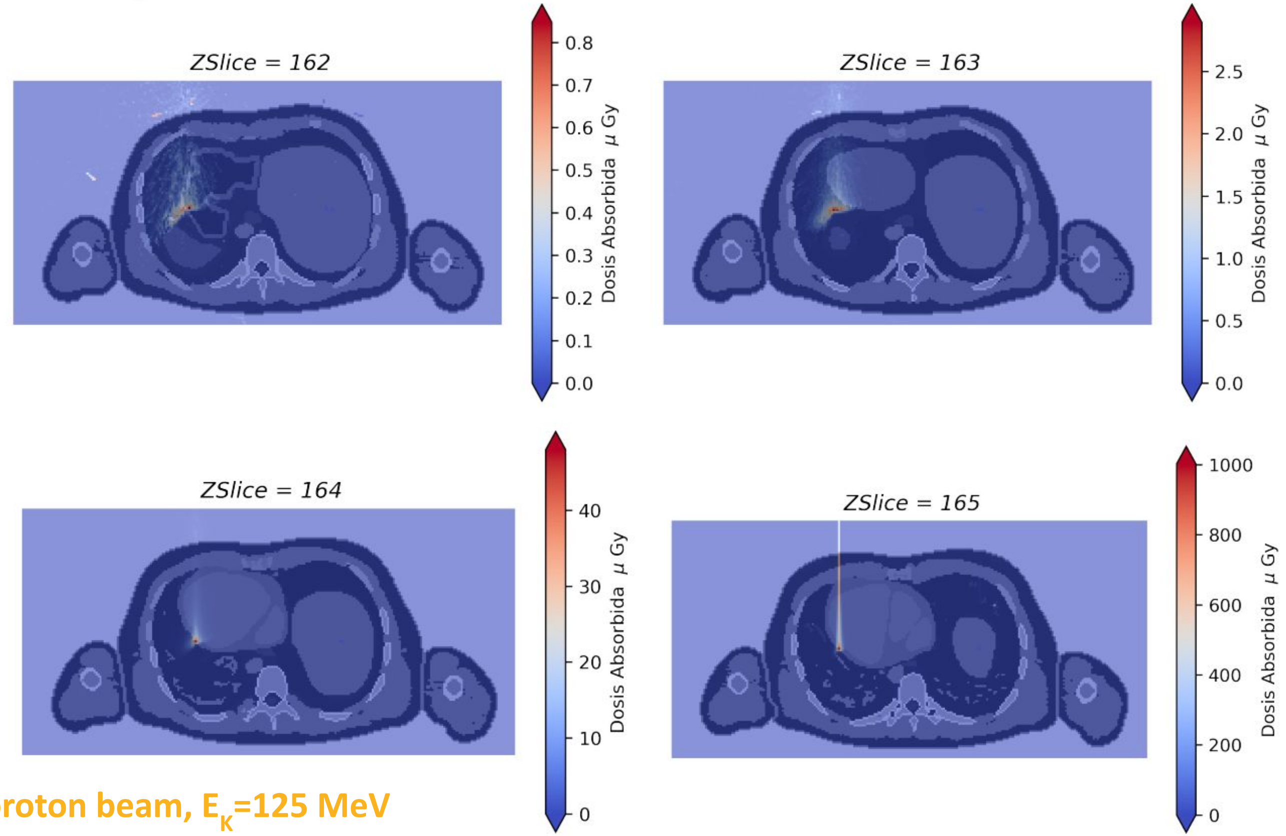

10^6 proton beam, E_K=125 MeV

Gracias